

Procainamide-SAHA fused inhibitors of hHDAC6 tackle multi-drug resistant malaria parasites

Flore Nardella^{1‡}, Ludovic Halby^{2‡}, Irina Dobrescu¹, Johanna Viluma², Corentin Bon^{2,3}, Aurélie Claes¹, Véronique Cadet-Daniel², Ambre Tafit², Camille Roesch⁴, Elie Hammam¹, Diane Erdmann^{2,3}, Melissa Mairet-Khedim⁴, Roger Peronet¹, Salah Mecheri¹, Benoit Witkowski⁴, Artur Scherf^{1*}, Paola B. Arimondo^{2*}

¹Unité Biologie des Interactions Hôte-Parasite, Département de Parasites et Insectes Vecteurs, Institut Pasteur, CNRS ERL 9195, INSERM Unit U1201, 25-28 Rue du Dr Roux, Paris 75015, France.

²Epigenetic Chemical Biology, Department of Structural Biology and Chemistry, Institut Pasteur, UMR n°3523, CNRS, 28 Rue du Dr Roux, Paris 75015, France.

³Ecole Doctorale MTCI ED563, Université de Paris, Sorbonne Paris Cité, Paris 75270, France

⁴Malaria Molecular Epidemiology Unit, Pasteur Institute in Cambodia, Phnom Penh 12201, Cambodia

KEYWORDS. *Histone deacetylase, DNA methylation, antimalarial, Plasmodium falciparum, parasite, in vivo, malaria, HDAC6 inhibitors, drug resistance.*

ABSTRACT: Epigenetic post-translational modifications are essential for human malaria parasite survival and progression through its life cycle. Here we present new functionalized SAHA derivatives that chemically combine the pan-histone deacetylase inhibitor SAHA with the DNA methyltransferase inhibitor procainamide. A 3- or 4-steps chemical synthesis was designed starting from cheap raw materials. Compared to the single drugs, the combined molecules showed superior activity in *Plasmodium* and a potent inhibition against human HDAC6, exerting no cytotoxicity in human cell lines. These new compounds are fully active in multi-drug resistant *Plasmodium falciparum* Cambodian isolates. They target transmission of the parasite by inducing irreversible morphological changes in gametocytes and inhibiting exflagellation. The compounds are slow-acting and have an additive antimalarial effect in combination with fast-acting epidrugs and dihydroartemisinin. The lead compound decreases parasitemia in mice in a severe malaria model. Taken together, this novel fused molecule offers an affordable alternative to current failing antimalarial therapy.

INTRODUCTION

Malaria is a parasitic disease that caused 229 million cases and 409.000 deaths in 2019 according to the WHO ¹. *Plasmodium falciparum* is responsible for the highest burden among the five *Plasmodium* species that infect humans, as it induces severe cases of cerebral malaria and/or multi-visceral failure, eventually leading to death. The absence of an efficient vaccine ², the increasing resistance of the mosquito vector to insecticides ³ and the escalation of treatment failures to first line antimalarial therapies (Artemisinin-based Combination Therapies, ACT) in South-East Asia ⁴⁻⁷ threaten the progress made in the management of the disease. Thus, new therapeutic options are needed to eradicate malaria. Novel candidate drugs should show high potency along with high selectivity over host cells, be active against multi-drug resistant strains, have oral bioavailability and be low cost.

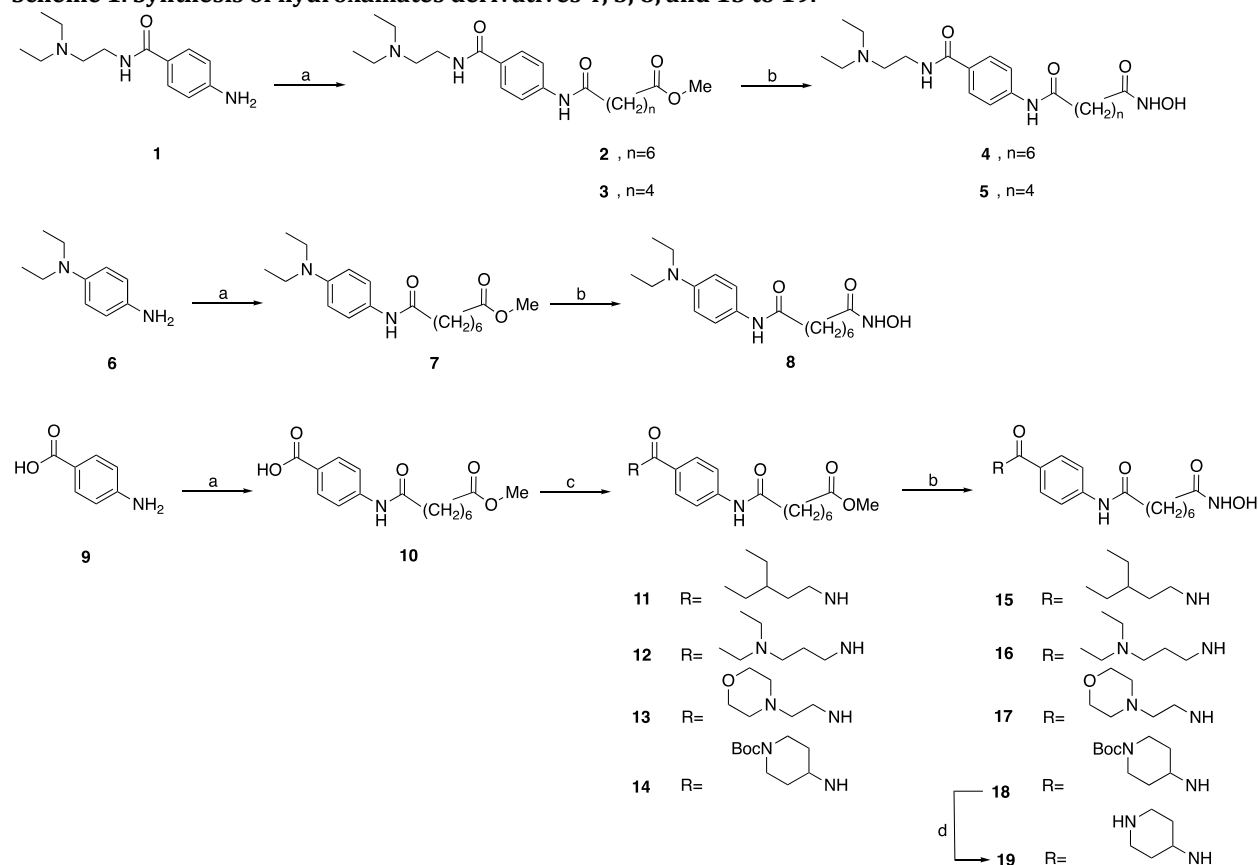
Epigenetic post-translational modifications (PTM) are essential for parasite survival and progression through all life cycle stages ⁸. The readers and writers of these PTM

are promising targets for new intervention strategies against *P. falciparum* but still little explored ⁸. Enzymes involved in histone post-translational modifications, such as methylation and acetylation, are involved in dynamic epigenetic processes modulating gene expression in concert with DNA methylation ⁹. Some of these enzymes are the target of FDA-approved drugs or drug candidates that are in clinical trials for cancer and neurological diseases ¹⁰. For parasite treatment, lysine acetylation of histones, regulated by histone lysine acetyltransferases (HAT) and lysine deacetylases (HDAC), have been explored ¹¹. While in mammals 18 HDACs form four major classes, only five enzymes are annotated in *Plasmodium*, and a sixth was recently identified ¹². PfHDAC1 belongs to the class I of HDACs, PfHDA1 and PfHDA2 belong to class II, and Sirtuins2A and B belong to class III. PfHDAC1 was first reported by Joshi *et al* in 1999 ¹³ and is involved in developmental processes such as schizogony, gametocytogenesis and hepatocyte invasion ¹⁴. It interacts with the chaperone protein PfHsp90 involved in chromatin remodeling ¹⁵. PfHDA2 regulates sexual commitment and

var gene monoallelic expression¹⁶, while PfHDA1 is not characterized yet. Sirtuins control the expression of heterochromatin-silenced virulence gene family¹⁷⁻¹⁹. Several studies demonstrated the ability of HDAC inhibitors to inhibit malaria parasite proliferation (reviewed extensively in^{11,20,21}), however, only few compounds have been reported to be specific for malaria and be highly potent²²⁻³⁰. To develop original and potent inhibitors, a promising strategy is dual inhibitors that combine two chemical moieties directed against different targets in one single molecule^{31,32}. Since a strong synergy between DNA methylation inhibitors and HDAC inhibitors is observed in cancer treatments^{33,34}, and we and others have shown that inhibitors of DNA methyltransferases (DNMTs) are able to inhibit *Plasmodium* growth both *in vitro* and *in vivo*^{35,36}, we merged the HDAC inhibitor SAHA

and the DNMT inhibitor procainamide³⁷ into the chimeric compound called Proca-SAHA/compound **4**. Proca-SAHA is active against *P. falciparum* asexual blood stage in the double digit nanomolar range, showing a nearly 50 times better selectivity for malaria *versus* human cells than SAHA alone. A Structure-Activity Relationship (SAR) study allowed further optimization resulting in compound **19** that delays the onset of parasitemia by *P. berghei* in mice when given *i.p.* in a model of severe malaria. We explored the pharmacological properties in the Intra-erythrocytic Developmental Cycle (IDC) and against *P. falciparum* sexual stages. The Proca-SAHA derivatives kill multi-drug resistant *P. falciparum* with high selectivity, inhibit predominantly the trophozoite stages and are active against gametocytes.

Scheme 1. Synthesis of hydroxamates derivatives 4, 5, 8, and 15 to 19.



(a) Methyl 8-chloro-8-oxooctanoate or methyl 6-chloro-6-oxohexanoate, TEA, DMF, RT, 18h. (b) NH_2OH 50%, MeOH, RT, 18h. (c) HATU, DiPEA, DMF, appropriate amine derivative, RT, 4h. d. TFA, RT, 1h.

RESULTS

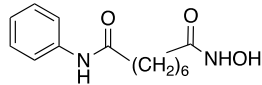
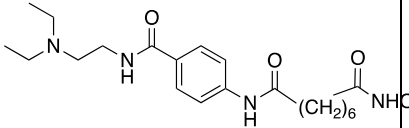
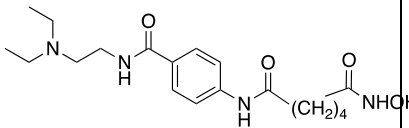
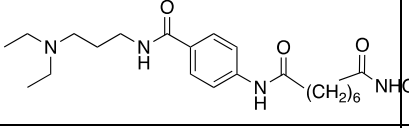
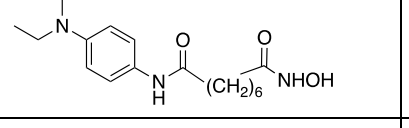
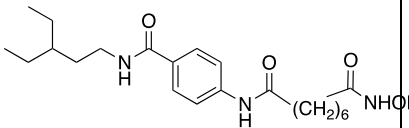
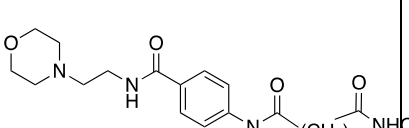
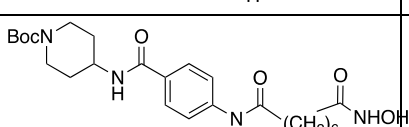
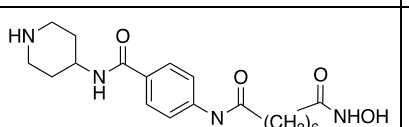
Design, synthesis and activity of Proca-SAHA derivatives

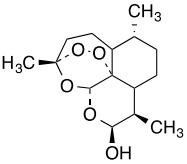
The scaffolds of the HDAC inhibitor SAHA and the DNMT inhibitor procainamide were fused in Proca-SAHA (compound **4**, Scheme 1). Compounds **4** and **5** were directly synthesized from procainamide **1** after coupling with methyl 6-chloro-6-oxohexanoate or methyl-8-chloro-

8-oxooctanoate followed by treatment with hydroxylamine in the presence of sodium hydroxide.

Compound **4** is four times more potent than SAHA against *P. falciparum* (IC_{50} s of 41 and 175nM, respectively). Interestingly, compound **4** is also 10-fold less toxic than SAHA in human liver HepG2 cells, and has low toxicity in leukemia cells HL60 (Table 1).

Table 1 - Inhibition activity of Proca-SAHA derivatives on the proliferation of asynchronous asexual cultures of *P. falciparum* NF54, cytotoxicity in human cell lines HepG2 and HL60 and activity against human and parasite extracts HDAC activity and recombinant hHDAC1, 2, 3, and 6. IC₅₀ values or percentage of inhibition at a given concentration are reported.

Name	Structure	Pf mean IC ₅₀ (nM)	Cytotoxicity (IC ₅₀ μM)		HDAC activity (IC ₅₀ μM)					
			Hep G2	HL60	hHDAC extracts	PfHDAC extracts	hHDAC 1	hHDAC 2	hHDAC 3	hHDAC6
SAHA		175±33	0.85 ±0.07	0.9 ±0.3	0.18 ±0.07	0.46 ±0.11	0.14 ±0.02	0.24 ±0.05	0.09 ±0.02	0.03 ±0.09
4/Proca SAHA		41±7	8.4 ±1.6	65% at 32μM	0.06 ±0.05	0.38 ±0.07	0.07 ±0.02	0.08 ±0.03	0.07 ±0.02	0.014 ±0.003
5		410±50	N.D.	N.D.	60% inh @ 1μM	N.D.	N.D.	N.D.	N.D.	N.D.
16		64±2	8.2 ±2.5	34±3	0.16 ±0.01	N.D.	N.D.	N.D.	N.D.	N.D.
8		239±13	2.4 ±0.9	2.7±1.3	0.21 ±0.08	N.D.	N.D.	N.D.	N.D.	N.D.
15		>500	> 100	>10	N.A.	N.D.	N.D.	N.D.	N.D.	N.D.
17		341±7	26 ±11	40% at 10μM	0.23 ±0.12	N.D.	N.D.	N.D.	N.D.	N.D.
18		467±10	~150 μM	2.5 ±0.8	N.A.	N.D.	N.D.	N.D.	N.D.	N.D.
19		52±12	~23 0μM	~100 μM	0.14 ±0.07	0.48 ±0.07	0.15 ±0.05	0.27 ±0.06	0.11 ±0.02	0.019 ±0.004

DHA		3±07	N.D.	N.D.	N.D.	N.D.	N.D.	N.D.	N.D.	N.D.
-----	---	------	------	------	------	------	------	------	------	------

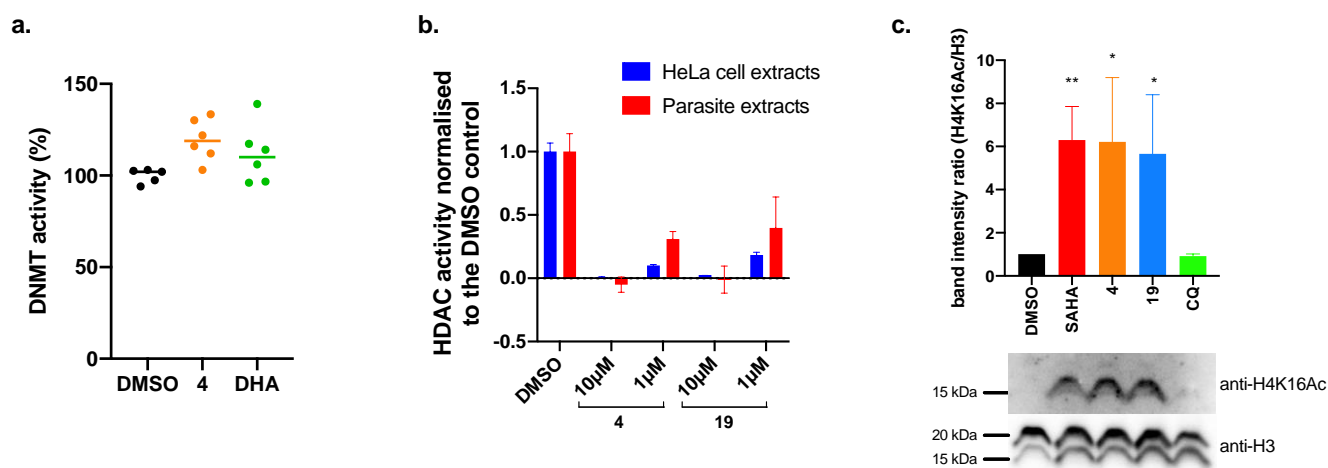
NA= no activity; N.D.= not determined

To further improve its activity and selectivity, we chemically modulated compound **4** using a rapid 3-step synthetic pathway to explore the importance of key substituent positions, with the exception of compound **19** that was obtained in 4-steps. We obtained 7 derivatives (Scheme 1). Compound **8** was obtained by coupling *N,N*-diethyl-*p*-phenylenediamine **6** with methyl 8-chloro-8-oxooctanoate following the same procedure as for compound **4**. Derivatives **15** to **18** were obtained from 4-aminobenzoic acid **9** that was first coupled to methyl 8-chloro-8-oxooctanoate. The resulting ester intermediate **10** was then reacted with the corresponding amine derivatives to obtain intermediates **11** to **14**, which were converted into the hydroxamic acids **15** to **18**. Compound **18** was finally treated with TFA to give compound **19**.

Shortening the linker between the phenyl group and the hydroxamic acid in compound **5** resulted in a loss of *P. falciparum* activity (Table 1), while increasing the linker

length by an atom between the diethylamine and the phenyl group (compound **16**) maintained the antimalarial activity. We thus focused on exploring the diethylaminoethylcarboxamide moiety and synthesized five derivatives. The loss of activity of compounds **15** and **8** demonstrates the importance of the terminal amine group and the amide group on the phenyl, respectively. Replacement of the diethylamine group by a morpholine group also resulted in a loss of activity (compound **17**). The cyclisation by coupling the piperidine to the carboxamide resulted in compound **19** that inhibited parasite growth in a similar manner as compound **4**, while the intermediated Boc-protected compound **18** was inactive. Interestingly, compound **19** revealed an excellent Selectivity Index (SI) compared to the cytotoxicity in human liver HepG2 and leukemia HL60 cell lines (Table 1).

Figure 1. Enzymatic activity of compounds 4 and 19. (a) Inhibition of *P. falciparum* nuclear extracts-mediated DNA methylation by compound 4 and dihydroartemisinin (DHA) at 32µM. Dots represents DNA methylation activity normalized to the control sample treated with DMSO obtained in two independent experiments ran in triplicate. (b) HDAC inhibition induced by compound 4 and 19 in HeLa cells and parasites extracts. Data represents the values obtained in two independent experiments ran in triplicate. (c) Hyper-acetylation of H4K16 following parasite treatment with SAHA and compounds 4 and 19. Trophozoite-stage parasites were treated for 4h with 10x the IC₅₀ of SAHA, compounds 4 and 19, and chloroquine (CQ) and western blotted (total extracts) using anti-H3 (loading control) and anti-H4K16ac antibodies. The histogram represents H4K16ac normalized with H3, as obtained from 3 independent experiments. Statistics: student's unpaired t-test in comparison to DMSO, *<0.05; **=0.0041.



Proca-SAHA derivatives target HDACs but not DNMTs

As we designed compound **4** to target DNMTs and HDACs, we assessed its activity in in-house DNMT³⁶ and HDAC enzymatic assays using *P. falciparum* extracts (Figure 1) and HeLa cells nuclear extracts (Figure 1b, Table 1). While compound **4** showed no activity against *P. falciparum* DNA methylation (Figure 1a) nor human DNMT3A methylation (data not shown), it inhibited

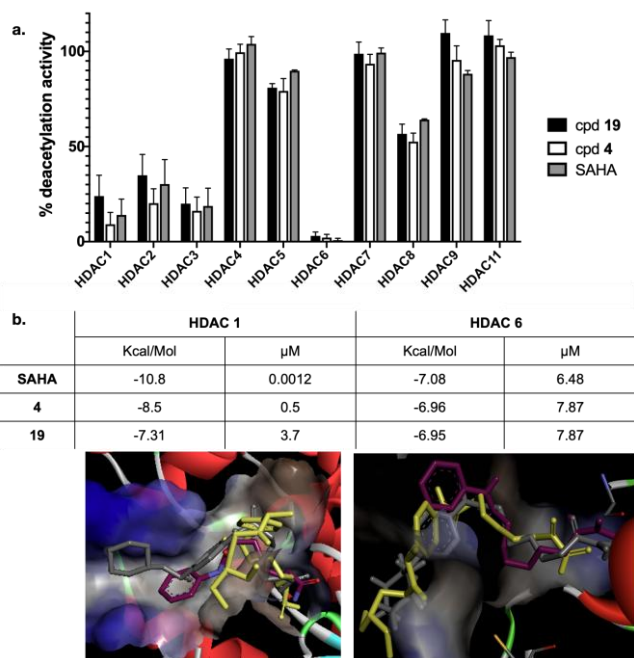
acetylation of histones in both human and *P. falciparum* extracts (Figure 1b). The optimized compound **19** efficiently inhibited histone acetylation in *P. falciparum* extracts (Figure 1b, IC₅₀ 480nM comparable to compound **4**, Table 1), but was less active on HeLa cell extracts than compound **4** (IC₅₀ of 140nM and 60nM, respectively).

Additionally, late stage cultures of *P. falciparum* were treated with **4** and **19** for 4h and the acetylation of lysine

16 of histone 4 (H4K16) was measured by western blot. Both compounds and SAHA increased the parasite H4K16 acetylation 6-folds compared to the DMSO and chloroquine controls (Figure 1c).

Finally, we profiled the human HDAC inhibition of compounds **4** and **19** (Figure 2a, Table 1). Both of them have an HDAC inhibition profile similar to SAHA and showed a strong activity against hHDAC6 (IC₅₀ of 14 and 19nM). In particular, **19** was less efficient in inhibiting hHDAC1 compared to compound **4** (Table 1). This was further confirmed by virtual Structure Activity Relationships (SAR) studies calculating the interaction score of compounds **4**, **19** and SAHA in the catalytic pocket of hHDAC1 and hHDAC6 crystal structures (Figure 2b, PDB: 5EDU and 5ICN, and Supplementary Figures 1 and 2). While the three compounds have comparable affinity for hHDAC6, compound **19** interacts to a lesser extent with hHDAC1 (Figure 2b). Indeed, according to the docking, the diethylamine and linker moieties of compound **4** fits in the hydrophobic pocket of hHDAC1 (Supplementary data Figure 1). The SAHA, smaller in size as it lacks the procainamide moiety, fits also, allowing hydrophobic interactions, coordination of the Zn²⁺ and a π-π interaction with Phe202. In the case of compound **19**, the steric hindrance of the piperidine prevents the correct positioning in the pocket resulting in a poor interaction thus explaining its lower inhibition efficacy against hHDAC1 (Table 1). The hHDAC6 pocket is larger and accommodates the fused derivatives allowing an optimal interaction with the Zn²⁺ and an additional interaction with Phe680 of the active site (Supplementary Figure 2). This suggests a possible different binding mode compared to SAHA, in which the phenyl Phe680 interacts with a phenylalanine closer to the active zinc. Interestingly, compound **19** showed also a decreased activity against hHDAC2. The higher activity of **19** for hHDAC6 could explain only in part the improved selectivity towards *Plasmodium* vs human cells, as SAHA shows a similar HDAC profile but, in contrast to **19**, is cytotoxic for human cells.

Figure 2. hHDAC selectivity. (a) Comparison of the inhibition of human HDACs for compounds 4 (white bars) and 19 (black bars) and SAHA (grey bars) at 1μM. (b) Docking studies. Compounds 4, 19 and SAHA were docked with Autodock in the resolved structures of hHDAC1 and hHDAC6 (PDB 5EDU and 5ICN). The best interaction scores are reported in kcal/mol and μM. Compound 19, represented in balls and sticks in grey, 4 in balls and sticks yellow and SAHA in ball and sticks purple were superimposed in the catalytic pocket of each HDAC using the best scored conformation. The hydrophobicity of the catalytic pocket is represented: from brown in the more hydrophobic part to blue in the more hydrophilic part. The enzyme secondary structure is highlighted: α-helices are in red and β-sheets in blue.



Proca-SAHA derivatives target the trophozoite stage in the IDC of *P. falciparum*

The lead compound **4** targets essentially the dividing stages of the IDC, with no effect on ring stage parasites and a mild effect against mature schizonts (Figure 3a). The most dramatic growth reduction (up to 85%) was obtained between 24 and 36hpi (hours post infection). Interestingly, the concentration used (3x or 10x IC₅₀) did not affect growth when parasites were treated for 6h.

Proca-SAHA derivatives are slow-acting compounds

The parasite reduction rate induced by 10x the IC₅₀ of compounds **4** and **19** is similar to that of the reference drug pyrimethamine (PYR), with one exception: the lag phase (time needed to achieve the maximum speed of action) is shorter (Figure 3b, Table 2). This confirms a different mode of action between Proca-SAHA derivatives and PYR³⁸. The phenotype obtained at each time point showed DNA-damage in the trophozoite stage, as the nuclei (in violet) appears disrupted (Figure 3c). Electron microscopy images of treated parasites show defective parasite division (Figure 3d-g): the merozoites are not individualized and nuclei are unstructured.

Table 2. Parasite Reduction Rate defined parameters³⁸.

	Lag phase (h)	Log(PRR)	PCT _{99.9%} (h)	Conclusion
4	0	3.80	40.3	slow
19	6	4.22	34.3	slow
DHA	0	5.12	21.2	fast-acting
PYR	24	3.57	44.1	slow

Lag phase= time needed to achieve the maximum speed of action

Log PRR= logarithm of the parasite reduction achieved over one cycle (48h)

PCT_{99.9%}= time needed to kill 99.9% of the initial parasite load

Compound 19 is additive with DHA and other epigenetic modulators

As compound **19** showed a slow-acting profile, we tested it in combination with DHA and two fast-acting epidrugs: the histone methyltransferase inhibitor BIX-01294 and the DNA methyltransferase inhibitor **70**^{36,39}. Compound **19** had an additive effect with all drugs tested (Figure 4a) as all the Fractional IC₅₀ (FIC) sums were below the value 1.5⁴⁰.

Proca-SAHA derivatives retain their activity against Cambodian multi-drug resistant isolates

An important feature for antimalarial drug candidates is to defeat drug-resistant parasites. Compounds **4** and **19** were tested on 50 Cambodian multi-drug resistant field isolates, bearing different molecular markers of resistance, for their ability to inhibit parasite proliferation. All isolates are resistant to chloroquine and pyrimethamine (called here “drug sensitive”) and present the following additional resistance phenotype: ART-R: artemisinin; ART-MQ: artemisinin and mefloquine; ART-PPQ: artemisinin and piperazine; ART-PPQ-AQ: artemisinin, piperazine and amodiaquine. Compounds **4** and **19** are active against all

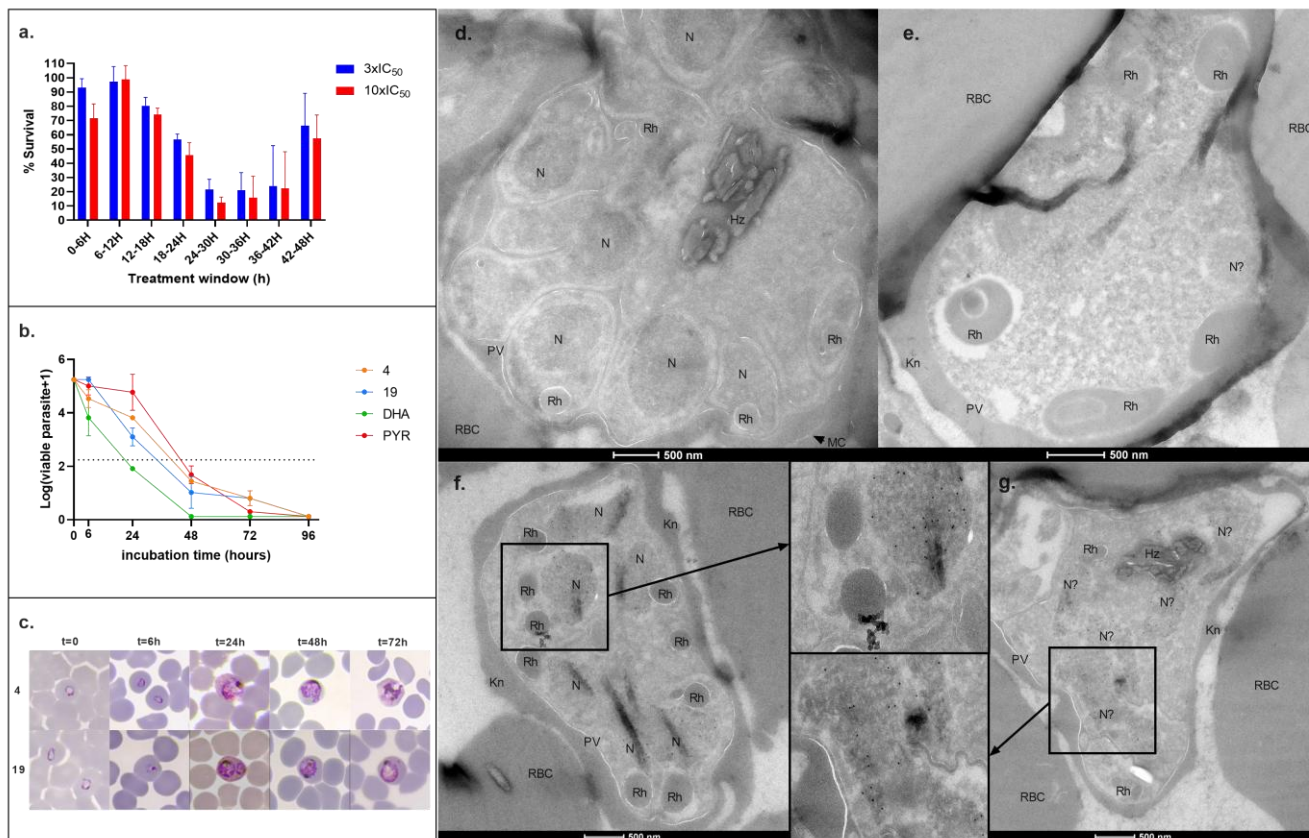
Figure 3. Activity against *P. falciparum* asexual blood stages. (a) Stage-specific activity in *P. falciparum* NF54 asexual cell cycle. Synchronized parasites were incubated with compound **4** for 6h, for 8 consecutive 6h periods covering the 48h cell cycle, at two different concentrations (3X and 10X IC₅₀). Survival rate was evaluated 72h after synchronization (n=3 independent experiments). (b) *In vitro* Parasite Reduction Rate (PRR). *P. falciparum* 3D7 culture containing mostly rings were incubated with compounds **4** and **19** or reference drugs (dihydroartemisinin DHA or pyrimethamine PYR) for different time windows (6h, 24h, 48h, 72h and 96h), washed, serially diluted in fresh RBC and allowed to grow for 3 weeks, then growth was assessed using the SYBR-green assay³⁸, N=1 experiment ran in duplicate. (c) Giemsa stained parasites showing representative phenotypes observed at the different time points of the PRR assay. (d to g) Transmission electron microscopy of schizont-stage *P. falciparum* parasites treated with compound **4**. (d) Control parasite treated with DMSO showing clearly defined merozoites and organelles. (e) Parasite treated with compound **4** showing a collapsed morphology, lacking internal organelles such as nucleus, having abnormal rhoptry structures and lacking well defined merozoites. (f and g) Parasites treated with DMSO (f) and compound **4** (g) stained with anti-H3 antibody labelled with 10nm colloidal gold to locate the chromatin. Middle panels show magnification of one merozoite (f) or a collapsed nuclei (g). RBC: red blood cell, Kn: Knob, MC: Maurer cleft, PV: parasitophorous vacuole, Hz: hemozoin crystals, N: nucleus, Rh: rhoptry.

Cambodian isolates tested (Figure 4b and Table 3), the IC_{50s} ranged between 35 and 168nM for compounds **4**, and 40 and 129nM for compound **19**. Mean IC₅₀ obtained with the 50 isolates are 77nM and 70nM respectively. Only one mean value differs significantly in the ART-PPQ-AQ group for compound **4** (p value=0.0188, Dunnett's multiple comparisons test).

Table 3. Mean, median, and interquartile range obtained in the Cambodian isolates.

	Mean±SD	Median	Interquartile range
4	76±28	70	57-86
19	70±19	66	58-84
MQ	30±19	27	17-39
desAQ	89±71	78	43-109

Values are given in nanomolar. N=50 isolates per group of treatment.



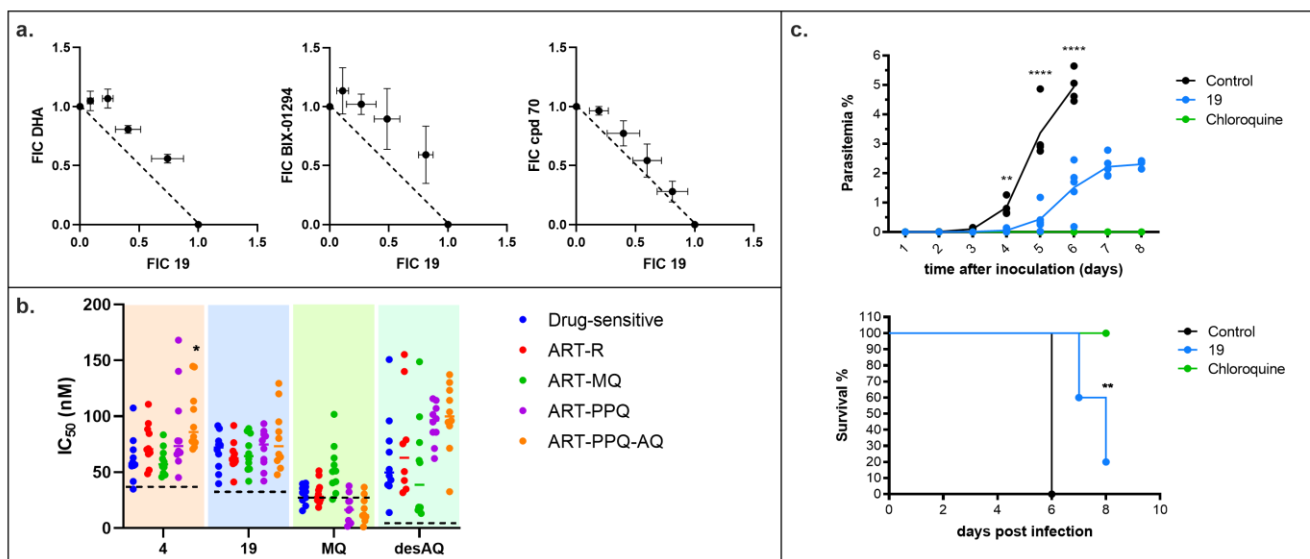
***In vivo* activity of compound 19 in the *P. berghei* cerebral malaria model**

Compound 19 showed good rat and human microsomal stability (100% remaining after 1h) and plasma stability (85% remaining after 2h) and was tested *in vivo* in a *P. berghei* severe malaria model. Twice-daily injections of 20mg/kg were chosen to maximize the efficacy as SAHA derivatives are known to have a rapid clearance²⁴. This dosage significantly delays growth of *P. berghei* (Figure 4c) during drug treatment (day 1 to 4). Survival was improved in the treated group: while all control mice died at day 6 with clinical signs of cerebral malaria, treated mice survived on average 2 days longer. No external signs of toxicity were observed in treated mice over the course of the treatment.

Proca-SAHA derivatives block transmission stages of *P. falciparum*

Stage IIb-III gametocytes were treated for 72 hours with the compounds. The morphology of treated gametocytes was analyzed daily by Giemsa-stained thin blood smears (Figure 5). At the highest concentration tested, up to 90% of gametocytes showed an abnormal morphology (Figure 5a-b): rounded or swollen, and presenting flagella-like extensions. In addition, we treated late stage gametocytes (IV-V) for 72h and performed an exflagellation assay (Figure 5c). Treatment with either 4 or 19 dramatically reduced the number of exflagellation centers at concentrations of 1 to 10 μ M, while SAHA had no activity at 1 μ M (Figure 5c, multiple comparison, ordinary one-way ANOVA).

Figure 4. Drug-interaction studies, activity against multi-drug resistant *P. falciparum* isolates and *in vivo* activity. (a) Isobolograms obtained for the combination of compound 19 with dihydroartemisinin, the histone methyltransferase inhibitor BIX-01294⁴¹ or the DNA methyltransferase inhibitor 70³⁶ in *P. falciparum* NF54 strain. (b) Activity against *P. falciparum* multi-resistant field isolates. IC₅₀s of compounds 4 and 19 obtained against Cambodian field isolates are plotted versus the type of resistance carried (ART-R: artemisinin resistant, ART-MQ: artemisinin and mefloquine resistant, ART-PPQ: artemisinin and piperazine resistant, ART-PPQ-AQ: artemisinin, piperazine and amodiaquine resistant). Mefloquine (MQ) and desethylamodiaquine (desAQ) are used as controls. The dotted lines represent the IC₅₀ obtained against the *P. falciparum* laboratory sensitive strain 3D7. Statistical analysis was done using two-way ANOVA (*p=0.0188). (c) *In vivo* activity of compound 19 in C57BL/6 mice infected with *P. berghei* ANKA. Five female mice per group were treated 2h after parasite inoculation, for 4 days, with a twice daily regimen of 20 mg/kg *i.p.* injections of compound 19 or vehicle control. Positive control mice received 25 mg/kg daily injections of chloroquine. Parasitemia and mortality were followed for 10 days. Statistics: Two-way ANOVA followed by Turkey's test, ** p=0.0021, ** p<0.0001; survival rate: Log rank (Mantel-cox) test, **p<0.005.**



DISCUSSION

DNA cytosine methylation and histone acetylation are epigenetic factors that contribute to developmental gene regulation in eukaryotes. Drugs that target these pathways show antimalarial activity^{42,43}. To exploit the synergistic activity of HDAC inhibitors with hypomethylating agents³³, we fused SAHA (Vorinostat) and procainamide together into compound **4**. SAHA is a FDA approved HDACi used for the treatment of cutaneous T-cell lymphoma, and procainamide is a DNA demethylating agent that slows down DNMT1 processivity upon binding to double-stranded DNA CpG islands in human cells³⁷. Our working hypothesis was that the two parts of the chimeric molecule **4** would cooperate together. Compound **4** inhibits *Plasmodium* histone acetylation like SAHA, but it does not inhibit hDNMT3A nor *Plasmodium* DNA methylation (Figure 1).

Dual inhibitors have already been explored for malaria treatment. For example Soumyanarayanan *et al.* combined SAHA to the epimodulator BIX-01294, targeting histone methyltransferase G9A⁴⁴, and obtained an IC_{50} of 95nM against the drug-sensitive strain 3D7 of *P. falciparum*, resulting less potent than BIX-01294 alone⁴¹. The dual compound was also 5-fold less active against the multi-drug resistant K1 strain and lacked selectivity ($SI_{3D7/HeLa}$ of 43). The chimeric compound **4** described here is 4-times more active than SAHA alone⁴⁵ and its SI towards *Plasmodium* is multiplied by 50. The chemical modulation of compound **4** resulted in compound **19**, which has a selectivity index 400-times higher than SAHA (Table 1). The chemical pathway was optimized in order to obtain the compounds in high yields at low cost.

An important feature of the Proca-SAHA derivatives is their selectivity against *Plasmodium* compared to human cells (Table 1). Partly, this could be linked to the high hHDAC6 inhibitory activity of compound **19**, as other inhibitors of hHDAC6 have been shown to be more selective for *Plasmodium* than human cells^{44,46,47}. However, as compound **19** shows a similar HDAC activity profile as SAHA but, in contrast to SAHA, is devoid of cytotoxicity

against human cells, other mechanisms are certainly involved in the activity of the procainamide-SAHA compound in parasites.

Noteworthy, PfHDAC1 is closely related to hHDAC1, while PfHDAC2 and 3 (also named HDA1 and HDA2) belong to class II HDACs, as does hHDAC6^{47,48}. As compounds **4** and **19** are very potent against hHDAC6, they might be targeting the activity of the class II *Plasmodium* HDACs. In humans, HDAC6 has two HDAC domains, is essentially cytoplasmic and is described to deacetylate alpha-tubulin on lysine 40⁴⁹. α K40 acetylation induces microtubules stabilization and can affect cell motility, cell signaling, and progression through the cell cycle⁵⁰. If PfHDAC2 and/or 3 have a similar activity as hHDAC6, it could explain the impaired division that we observe as well as the aberrant phenotype in gametocytes (Figures 3d-g and 5), as gametocytes have a very structured and stage-evolving cytoskeleton⁵¹. Also, we cannot exclude that the hyperacetylation of histones upon treatment is partly responsible for this phenotype. Further work will focus on deciphering the mode of action of compound **19** that can result in a potent chemical tool to study the role of this less-characterized HDAC activity in *Plasmodium*.

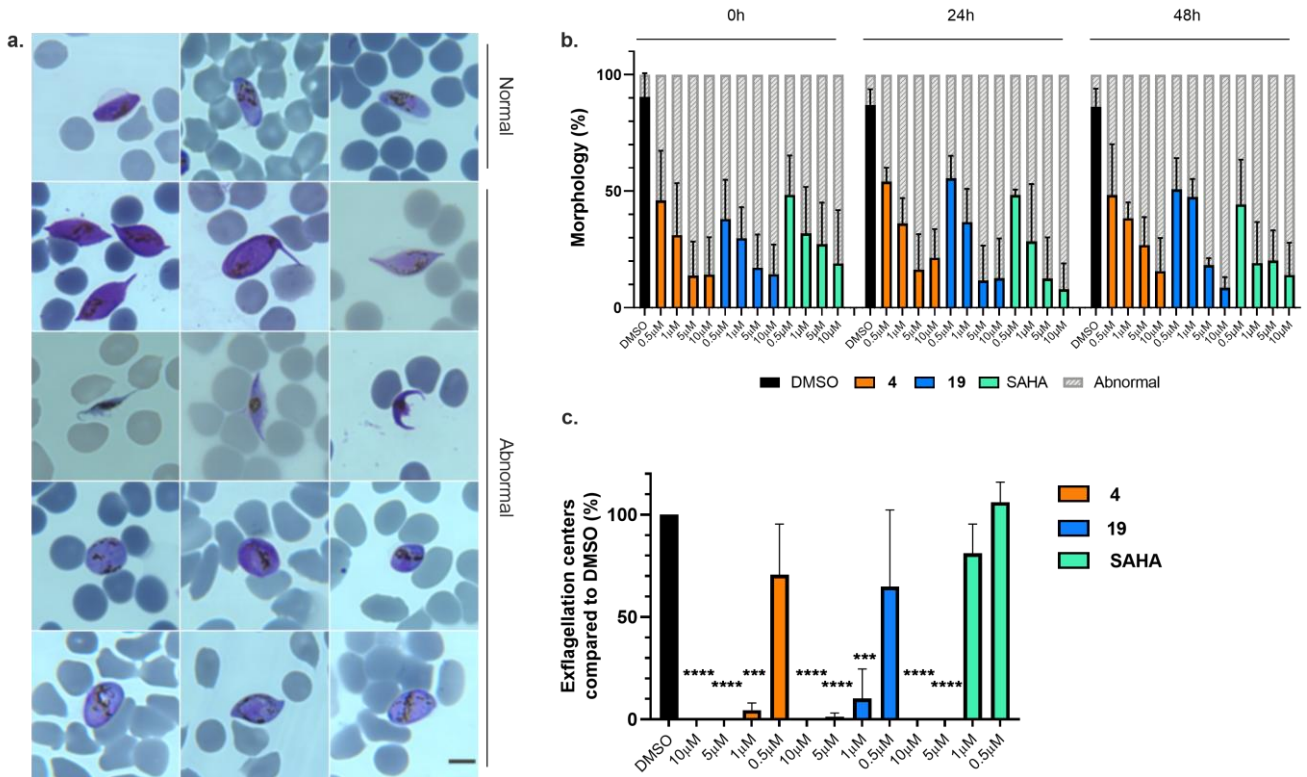
Proca-SAHA derivatives remain highly active against Cambodian multi-drug resistant field isolates, as no cross-resistance was observed with 50 isolates that carry multi-drug resistance to artemisinin, mefloquine, piperazine and/or amodiaquine (Figure 4b). In the literature two studies of HDACi mentions the use of field isolates from Gabon⁴⁶ and Indonesia⁵², however only isolates resistant to chloroquine were studied. Koehne *et al*⁴⁶ reported 1 to 3-fold increase in IC_{50} values compared to the laboratory 3D7 strain, in agreement with what we observed for compounds **4** and **19**, whereas Marfurt *et al*⁵² reported median IC_{50} values ranging from 20 to 35 times the value found with the 3D7 strain, although the values were determined *ex vivo* so they are difficult to compare with our results.

Interestingly, Kanyal *et al.* reported that artemisinin resistant strains have different patterns of HAT and HDAC RNA expression^{12,53}. In early stages of the IDC, PfHDAC1

and PfCHD1 (chromodomain-helicase-DNA-binding protein 1) are strongly downregulated in artemisinin-resistant strains, inducing a decrease in parasite metabolism and a dormancy phenotype, while PfHDA1 and PfHDA2 are mostly overexpressed. This HDAC deregulation is less pronounced in the trophozoite stage

^{12,53} that is the stage targeted by compounds **4** and **19**, which might explain the conserved antiproliferative activity against artemisinin-resistant strains that we observe.

Figure 5. Activity against *P. falciparum* gametocytes and gametes. (a) Frequently encountered morphologies observed in Giemsa-stained gametocytes after 72h treatment with compounds **4, **19** or SAHA at stage IIb-III. Gametocytes are swollen, rounded or present flagella-like extensions. Scale bar represents 5µm. (b) Quantification of gametocytes showing an abnormal morphology (as pictured in (a)). Time points are post drug removal. Data showed are the mean and SD of three independent experiments. (c) Exflagellation centers compared to DMSO. Stage VI-V gametocytes were treated for 72h with compounds **4**, **19** or SAHA, washed and differentiated into gametes. Data represent the mean and SD of two independent experiments. Statistics: Two-way ANOVA, Dunett's multiple comparison test, *** p<0.001; **** p<0.0001.**



Efficient antimalarial drugs need to block transmission. Early gametocytes treated with up to 10µM of proca-SAHA derivatives for 72h have an abnormal morphology, even if they are still viable as their mitochondria is active (data not shown). The 72h treatment of late stage gametocytes did not induce a phenotype, nor decreased the parasitemia. This absence of activity is in contrast to HDACi reported in the literature for having submicromolar IC₅₀s against late stage gametocytes ^{25,54}. Perhaps increased potency for class II HDACs decreases the activity against this stage. Of interest to block transmission, compounds **4** and **19** significantly reduce the exflagellation at a concentration as low as 1µM, in contrast to reports from Trenholme, *et al.* who found that SAHA and TSA, both HDACi, have no activity on exflagellation ⁵⁴. However, they used a 15min incubation instead of 72h. In our experiments, SAHA has no activity at 1µM, but inhibits exflagellation at a concentration of 5µM, showing that **4** and **19** are more

potent on this stage. These observations highlight the potential to use these possible inhibitors of *P. falciparum* class II HDACs in further studies.

Finally, in an *in vivo* severe malaria model compound **19** delays the onset of parasitemia and increases mice survival. This outcome is better than what was observed with SAHA in a non-severe malaria murine model ⁴⁵. Even if the *in vivo* results are very encouraging for future drug development, we will need to improve the plasma stability of compound **19**. Multiple studies report partial *in vivo* efficacy of HDACi but none achieved cure as a monotherapy ^{22-24,27}. Also, we report here the first example of HDACi combination with epidrugs or with dihydroartemisinin against *P. falciparum* resulting in an additive effect. Further work is needed to evaluate the impact of these combinations *in vivo* as this finding could lead to novel ACTs or non-artemisinin combination therapies.

CONCLUSIONS

The fusion of the histone deacetylase inhibitor SAHA and the DNMT inhibitor procainamide into a single compound, Proca-SAHA, resulted in an original family of antimalarials that is highly potent and selective for *Plasmodium*. Interestingly, the lead compound **19** is highly potent against hHDAC6 and shows no cytotoxicity in human cancer cells. The synthesis itself is low-cost thus favoring affordable drug development. Importantly, Proca-SAHA derivatives are highly active against multiple *P. falciparum* isolates from Cambodia, the epicenter of malaria drug-resistance, which makes them excellent drug candidates. The Proca-SAHA derivatives have an additive effect in combination with DHA and two fast-acting epidrugs (histone- and DNA-methyltransferases inhibitors). They have the potential to block transmission since they induce an abnormal morphology in gametocytes and inhibit the formation of male gametes. *In vivo*, lead compound **19** delays the onset of parasitemia when injected intraperitoneally in a severe model of malaria. Further work will focus on optimizing the pharmacokinetic properties and testing drug combinations in order to improve their potency *in vivo*, in addition to deciphering the HDAC targets in *Plasmodium*.

EXPERIMENTAL SECTION

Chemical synthesis

All chemicals were from Sigma-Aldrich, Alfa Aesar and FluoChem. NMR experiments were recorded on an Agilent DirectDrive 500 spectrometer (Agilent Technologies, Santa Clara) with a proton resonating frequency of 499.8MHz. Spectra were recorded using Vnmrj 4.2A (Agilent Technologies). Chemical shifts are given in ppm. Coupling constants J are measured in Hz. Splitting patterns are designed as follows: s, singlet; bs broad singlet; d, doublet; bd broad doublet; t, triplet; brt, broad triplet; dd, doublet of a doublet; m, multiplet; ddd, doublet of a doublet of a doublet; q, quartet; quint, quintet; sext, sextet. HRMS analysis were performed on a Q Exactive mass Spectrometer (ThermoFisher) using direct injection. Samples were previously dissolved in a mix of water and acetonitrile (50/50) and 0.1% of formic acid. Full scans (150-2000Da) were acquired in positive ion mode with a resolution of 70,000. The purity of all final compounds was verified to be higher than 95% using reversed-phase HPLC system (Agilent 1200 series) equipped with a diode-array detector on a C18 reverse phase column (Kromasil, 5 μ m, 100 \AA ; 4.6 \times 150mm) at a flow rate of 1mL.min⁻¹ with a linear gradient of acetonitrile in 10mM triethylammonium acetate buffer over 20min. (5 to 95% CH₃CN).

Synthesis of compounds **4** and **8**.

Methyl 8-(4-(2-(diethylamino)ethylcarbamoyl)phenylamino)-8-oxooctanoate (**2**)

Methyl 8-chloro-8-oxooctanoate (156 μ L, 1.1mmol) was added to a solution of procainamide hydrochloride salt (**1**) (271mg, 1.0mmol) in DMF (10mL) and TEA (418 μ L, 3.0mmol). The reaction mixture was stirred at RT for 4h and then quenched with methanol. Ethyl acetate (100mL) was added and the organic phase was washed with a 10% K₂CO₃ solution, brine and dried over Na₂SO₄. The solvents were evaporated and the residue was purified by silica gel flash chromatography using

a linear gradient of DCM/methanol (0 to 10%, MeOH) to give **2** as a yellow oil (381mg, 0.94 mmol, 94%).

¹H NMR (500MHz; CDCl₃) δ 8.45 (s, 1H), 8.83 (d, *J* = 8.7Hz, 2H), 7.78 (brt, *J* = 5.9Hz, 1H), 8.67 (d, *J* = 8.7Hz, 2H), 3.67 (s, 3H), 3.61 (q, *J* = 5.7Hz, 2H), 2.91 (t, *J* = 5.4Hz, 2H), 2.82 (q, *J* = 7.2Hz, 4H), 2.40 (t, *J* = 7.7Hz, 4H), 2.32 (t, *J* = 7.4Hz, 4H), 1.72 (quint, *J* = 7.3Hz, 2H), 1.62 (quint, *J* = 7.2Hz, 2H), 1.41-1.31 (m, 4H), 1.92 (t, *J* = 7.8Hz, 6H).

¹³C NMR (125MHz; CDCl₃) δ 174.3, 172.0, 167.1, 141.5, 129.0, 128.1, 119.2, 52.1, 51.5, 47.5, 37.4, 36.5, 33.9, 28.8, 28.7, 25.3, 24.7, 10.6.

HRMS-ESI(m/z) calculated for C₃₃H₄₆N₇O₈ [M+H]⁺: 406.2700; Found: 406.2723.

Methyl 6-((4-(2-(diethylamino)ethylcarbamoyl)phenyl)amino)-6-oxohexanoate (**3**)

Following the same procedure, **3** was synthesised starting from procainamide hydrochloride salt (300mg, 1.10mmol) and methyl 6-chloro-6-oxohexanoate (236 μ L, 1.32mmol). It was obtained as a pale yellow powder (407mg, 1.08mmol, 98%).

¹H NMR (500MHz, DMSO-*d*₆) δ : 10.07 (s, 1H), 8.21 (t, *J* = 5.7 Hz, 1H), 7.78 - 7.72 (m, 2H), 7.66 - 7.60 (m, 2H), 3.56 (s, 3H), 3.31 - 3.23 (m, 2H), 2.55 - 2.43 (m, 6H), 2.32 (t, *J* = 6.9 Hz, 4H), 1.63 - 1.45 (m, 4H), 0.94 (t, *J* = 7.1 Hz, 6H).

¹³C (125MHz, DMSO-*d*₆) δ : 173.2, 171.3, 165.5, 141.7, 128.9, 127.9, 118.1, 51.5, 51.2, 46.8, 37.5, 36.0, 33.0, 24.4, 24.0, 11.9.

HRMS-ESI(m/z) calculated for C₂₀H₃₂N₃O₄ [M+H]⁺: 378.2387; Found: 378.2370.

N-(4-(2-(diethylamino)ethylcarbamoyl)phenyl)-N⁸-hydroxyoctanediamide (**4**)

Compound **2** (82mg, 0.20mmol) was suspended in a solution of 50% of hydroxylamine and methanol (1:1) and the mixture was stirred at RT overnight. The solvents were removed and the residue was purified by reversed phase chromatography using a linear acetonitrile gradient with 0.01% of TEA (0 \rightarrow 80% CH₃CN) to afford **4** as a white powder (52mg, 0.13mmol, 64%).

¹H NMR (500MHz, DMSO-*d*₆) δ : 10.32 (brs, 1H), 10.08 (s, 1H), 8.66 (brs, 1H), 8.22 (brt, *J* = 5.8Hz, 1H), 7.77 (d, *J* = 8.7Hz, 2H), 7.65 (d, *J* = 8.7Hz, 2H), 3.29 (dt, *J* = 8.7, 5.7Hz, 2H), 2.56-2.46 (m, 7H), 2.31 (t, *J* = 7.7Hz, 4H), 1.94 (t, *J* = 7.4Hz, 4H), 1.58 (quint, *J* = 7.1Hz, 2H), 1.50 (quint, *J* = 7.1Hz, 2H), 1.34-1.22 (m, 4H), 1.00 (t, *J* = 7.1Hz, 6H).

¹³C NMR (125MHz; DMSO-*d*₆) δ : 172.1, 169.6, 166.0, 142.2, 129.2, 128.3, 118.6, 51.9, 47.2, 37.9, 36.8, 32.7, 28.8, 25.5, 24.3, 12.3.

HRMS-ESI(m/z) calculated for C₃₃H₄₆N₇O₈ [M+H]⁺: 407.2653; Found: 407.2639.

N¹-(4-((2-(diethylamino)ethylcarbamoyl)phenyl)-N⁶-hydroxyadipamide (**5**)

5 was synthesised following the same procedure as **4** starting from **3** (100mg, 0.26mmol). It was obtained as a white powder (87mg, 0.23mmol, 88%).

¹H NMR (500MHz, DMSO-*d*₆) δ : 10.33 (s, 1H), 10.06 (s, 1H), 8.66 (s, 1H), 8.20 (t, *J* = 5.7 Hz, 1H), 7.77 - 7.72 (m, 2H), 7.63 (d, *J* = 8.5 Hz, 2H), 3.30 - 3.23 (m, 2H), 2.54 - 2.45 (m, 7H), 2.30 (t, *J* = 6.9 Hz, 2H), 1.96 (t, *J* = 6.9 Hz, 2H), 1.60 - 1.47 (m, 4H), 0.94 (t, *J* = 7.1 Hz, 6H).

¹³C (125MHz; DMSO-*d*₆) δ : 171.4, 168.9, 165.5, 141.7, 128.9, 127.9, 118.1, 51.6, 46.8, 37.5, 36.2, 32.2, 24.8, 24.7, 12.0.

HRMS-ESI(m/z) calculated for C₁₉H₃₁N₄O₄ [M+H]⁺: 379.2340; Found: 378.2323.

Methyl 8-((4-(diethylamino)phenyl)amino)-8-oxooctanoate (**7**)

Methyl 8-chloro-8-oxooctanoate (156 μ L, 1.1mmol) was added to a solution of *N,N*-diethyl-*p*-phenylenediamine **6** (180mg, 1.1mmol) in DMF (10mL) and TEA (418 μ L, 3.0mmol). The reaction mixture was stirred at RT for 4h and then quenched with methanol. Ethyl acetate (100mL) was added and the organic phase was washed with a 10% K₂CO₃ solution and brine and dried over Na₂SO₄. The solvents were evaporated and the residue was purified by silica gel flash chromatography using a linear gradient of DCM/methanol (0 to 10%, MeOH) to give **7** as a dark violet foam (257mg, 0.77mmol, 70%).

¹H NMR (500MHz, DMSO-*d*₆) δ : 9.47 (s, 1H), 7.33 (d, *J* = 9.1 Hz, 2H), 6.59 (d, *J* = 9.1 Hz, 2H), 3.57 (s, 3H), 3.26 (q, *J* = 7.0 Hz, 4H), 2.29 (t, *J* = 7.4 Hz, 2H), 2.21 (t, *J* = 7.5 Hz, 2H), 1.59 – 1.47 (m, 4H), 1.31 – 1.24 (m, 4H), 1.04 (t, *J* = 7.0 Hz, 6H).

¹³C (125MHz, DMSO-*d*₆) δ : 173.3, 170.2, 143.8, 128.3, 121.0, 112.0, 51.2, 43.8, 36.1, 33.2, 28.3, 28.2, 25.1, 24.3, 12.4.

HRMS-ESI(*m/z*) calculated for C₁₉H₃₁N₂O₃ [M+H]⁺: 335.2329; Found: 335.2307.

***N*¹-(4-(diethylamino)phenyl)-*N*⁸-hydroxyoctanediamide (**8**)**

Compound **7** (80mg, 0.24mmol) was suspended in a solution of 50% of hydroxylamine and methanol (1:1) and the mixture was stirred at RT for 24h. The solvents were removed and the residue was purified by reversed phase chromatography using a linear acetonitrile gradient with 0.01% of TEA (0→80% CH₃CN) to afford **8** as a white powder (35mg, 0.10mmol, 42%).

¹H NMR (500MHz, DMSO-*d*₆) δ : 10.32 (s, 1H), 9.47 (s, 1H), 8.64 (s, 1H), 7.73 (d, *J* = 9.0 Hz, 2H), 6.59 (d, *J* = 8.9 Hz, 2H), 3.26 (q, *J* = 7.0 Hz, 4H), 2.21 (t, *J* = 7.4 Hz, 2H), 1.93 (t, *J* = 7.4 Hz, 2H), 1.51 (dp, *J* = 31.5, 7.1 Hz, 4H), 1.25 (m, 4H), 1.04 (t, *J* = 7.0 Hz, 6H).

¹³C (125MHz, DMSO-*d*₆) δ : 170.2, 169.1, 142.2, 127.1, 120.2, 112.0, 43.8, 36.2, 32.3, 28.5, 28.4, 25.2, 25.1, 12.4.

HRMS-ESI(*m/z*) calculated for C₁₈H₃₀N₃O₃ [M+H]⁺: 336.2282; Found: 336.2255.

Synthesis of 4-(8-(hydroxyamino)-8-oxooctanamido)benzoic acid (10**)**

Methyl 8-chloro-8-oxooctanoate (2.52mL, 17.8mmol) was added to a solution of *p*-aminobenzoic acid **9** (2.23g, 16.2mmol) and triethylamine (6.76mL, 48.6mmol) in DMF (20ml) under argon. The reaction mixture was stirred at RT overnight and then quenched with methanol. Ethyl acetate (100mL) was added and the mixture was washed with a 1M HCl solution (3 \times 200mL) and with brine (2 \times 200mL). The organic layer was dried over MgSO₄ and the solvents were evaporated. The residue was purified by silica gel flash chromatography using a linear gradient of DCM/methanol (0 to 10%, MeOH) to give **10** as a white powder (4.08g, 13.3mmol, 82%).

¹H NMR (500MHz; DMSO-*d*₆) δ : 12.67 (s, 1H), 10.15 (s, 1H), 7.86 (d, *J* = 8.7 Hz, 2H), 7.69 (d, *J* = 8.5 Hz, 2H), 3.57 (d, *J* = 1.2 Hz, 3H), 2.36 – 2.25 (m, 4H), 1.55 (m, 4H), 1.29 (m, 4H).

¹³C NMR (125MHz; DMSO-*d*₆) δ : 173.3, 171.8, 166.9, 143.3, 130.3, 124.9, 118.2, 51.2, 36.4, 33.2, 28.3, 28.2, 24.8, 24.3.

HRMS-ESI(*m/z*) calculated for C₁₆H₂₀NO₅ [M-H]⁺: 306.1347; Found: 306.1349.

General procedure for the synthesis of compounds **11 to **14**:**

DIPEA (3eq.) was added to a solution of a **10** (100mg, 0.33mmol) and HATU (1.5eq.) in DMF (0.1M), and the mixture was stirred at RT for 10min then the corresponding amine

(1.5eq.) was added. The reaction mixture was stirred at RT for 4h. Ethyl acetate was added to the mixture and washed with water, a 1M HCl solution and brine. The solvent was removed and the residue was purified by silica gel flash chromatography using a linear gradient of DCM/methanol (0 to 10%, MeOH) to give the desired product.

Methyl 8-((4-((3-ethylpentyl)carbamoyl)phenyl)amino)-8-oxooctanoate (11**)** was obtained as a pale yellow powder (88mg, 0.22mmol, 67%).

¹H NMR (600MHz; DMSO-*d*₆) δ : 10.06 (s, 1H), 8.29 (t, *J* = 5.6 Hz, 1H), 7.78 (m, 2H), 7.65 (m, 2H), 3.58 (s, 3H), 3.27 – 3.21 (m, 2H), 2.31 (dt, *J* = 11.5, 7.4 Hz, 4H), 1.56 (dq, *J* = 31.7, 8.0, 7.0 Hz, 4H), 1.450-1.44 (m, 2H), 1.34 – 1.22 (m, 9H), 0.84 (t, *J* = 7.3 Hz, 6H).

¹³C NMR (151MHz; DMSO-*d*₆) δ : 173.8, 172.0, 165.9, 142.2, 129.4, 128.4, 118.6, 51.6, 38.0, 37.6, 36.8, 33.7, 32.7, 28.8, 28.7, 25.4, 25.3, 24.8, 11.1.

HRMS-ESI(*m/z*) calculated for C₂₃H₃₇N₂O₄ [M+H]⁺: 405.2748; Found: 405.2738.

Methyl 8-((4-((3-(diethylamino)propyl)carbamoyl)phenyl)amino)-8-oxooctanoate (12**)** was obtained as a pale yellow powder (99mg, 0.24mmol, 73%).

¹H NMR (500MHz; DMSO-*d*₆) δ : 10.05 (s, 1H), 8.37 (t, *J* = 5.5 Hz, 1H), 7.76 (d, *J* = 8.4 Hz, 2H), 7.64 (d, *J* = 8.4 Hz, 2H), 3.57 (s, 3H), 3.25 (q, *J* = 6.6 Hz, 2H), 2.48 – 2.38 (m, 6H), 2.30 (m, 4H), 1.66 – 1.47 (m, 6H), 1.29 (m, 4H), 0.93 (t, *J* = 7.1 Hz, 6H).

¹³C NMR (125MHz; DMSO-*d*₆) δ : 174.4, 171.5, 164.8, 141.7, 129.6, 127.8, 118.7, 51.7, 50.3, 46.3, 38.0, 36.4, 33.2, 28.2, 26.6, 24.8, 24.3, 11.7.

HRMS-ESI(*m/z*) calculated for C₂₃H₃₈N₃O₄ [M+H]⁺: 420.2857; Found: 420.2847.

Methyl 8-((4-((2-morpholinoethyl)carbamoyl)phenyl)amino)-8-oxooctanoate (13**)** was obtained as a white powder (95mg, 0.23mmol, 70%).

¹H NMR (500MHz; DMSO-*d*₆) δ : 10.06 (s, 1H), 8.25 (t, *J* = 5.7 Hz, 1H), 7.77 (d, *J* = 8.5 Hz, 2H), 3.57 (m, 7H), 7.65 (d, *J* = 8.5 Hz, 2H), 3.36 (m, 2H), 2.42 (m, 6H), 2.30 (m, 4H), 1.55 (m, 4H), 1.29 (m, 4H).

¹³C NMR (125MHz; DMSO-*d*₆) δ : 173.3, 171.6, 166.0, 141.8, 128.7, 127.3, 117.7, 66.2, 57.4, 53.3, 51.2, 36.5, 36.4, 33.2, 28.3, 28.2, 24.8, 24.3.

HRMS-ESI(*m/z*) calculated for C₂₂H₃₄N₃O₅ [M+H]⁺: 420.2493; Found: 420.2486.

***tert*-Butyl 4-(4-(8-methoxy-8-oxooctanamido)benzamido)piperidine-1-carboxylate (**14**)** was obtained as a white powder (382mg, 0.78mmol, 96%).

¹H NMR (500MHz; DMSO-*d*₆) δ : 10.04 (s, 1H), 8.10 (d, *J* = 7.9 Hz, 1H), 7.79 – 7.74 (m, 2H), 7.65 – 7.60 (m, 2H), 4.01 – 3.79 (m, 3H), 3.56 (s, 3H), 2.89 (m, 4H), 2.28 (m, 4H), 1.83 – 1.67 (m, 2H), 1.61 – 1.47 (m, 4H), 1.39 (s, 12H), 1.34-1.20 (m, 4H).

¹³C (125MHz, DMSO-*d*₆) δ : 173.3, 171.6, 165.0, 153.9, 141.8, 128.8, 128.1, 118.0, 78.6, 51.2, 46.4, 36.3, 33.2, 31.4, 28.3, 28.2, 28.1, 28.0, 24.8, 24.3.

HRMS-ESI(*m/z*) calculated for C₂₆H₄₀N₃O₆ [M+H]⁺: 490.2912; Found: 490.2904.

General procedure for the synthesis of compounds 15 to 18:

The corresponding ester derivative (11 to 14) was suspended in a solution of 50% of hydroxylamine and methanol (1:1) and the mixture was stirred at RT for 24h. The solvent was removed and the residue was purified by reversed phase chromatography using a linear acetonitrile gradient with 0.01% of TEA (0→80% CH₃CN) to afford the desired hydroxamic acid derivative.

***N*¹-4-((3-ethylpentyl)carbamoyl)phenyl)-*N*⁸-hydroxyoctanediamide (15)** was obtained from 11 (64mg, 0.16mmol) as a white powder (47mg, 0.12mmol, 72%).

¹H NMR (500MHz; DMSO-*d*₆) δ: 10.32 (s, 1H), 10.05 (s, 1H), 8.64 (s, 1H), 8.27 (t, *J* = 5.6 Hz, 1H), 7.79 – 7.73 (m, 2H), 7.63 (d, *J* = 8.6 Hz, 2H), 3.26 – 3.19 (m, 2H), 2.31 (t, *J* = 7.4 Hz, 2H), 1.93 (t, *J* = 7.4 Hz, 2H), 1.57 (p, *J* = 7.4 Hz, 2H), 1.53 – 1.41 (m, 4H), 1.34 – 1.20 (m, 9H), 0.83 (t, *J* = 7.3 Hz, 6H).

¹³C NMR (125MHz; DMSO-*d*₆) δ: 171.6, 169.1, 165.4, 141.7, 129.0, 127.9, 118.1, 37.6, 37.1, 36.4, 32.2, 28.4, 25.0, 24.9, 24.8, 10.6.

HRMS-ESI(*m/z*) calculated for C₂₂H₃₆N₃O₄ [*M+H*]⁺: 406.2700; Found: 406.2692.

***N*¹-4-((3-(diethylamino)propyl)carbamoyl)phenyl)-*N*⁸-hydroxyoctanediamide (16)** was obtained from 12 (78mg, 0.19mmol) as a white powder (45mg, 0.11mmol, 58%).

¹H NMR (500MHz; DMSO-*d*₆) δ: 10.32 (s, 1H), 10.06 (s, 1H), 8.66 (s, 1H), 8.37 (t, *J* = 5.6 Hz, 1H), 7.76 (d, *J* = 8.5 Hz, 2H), 7.64 (d, *J* = 8.4 Hz, 2H), 3.25 (q, *J* = 6.6 Hz, 2H), 2.44 (m, 6H), 2.31 (t, *J* = 7.5 Hz, 2H), 1.93 (t, *J* = 7.4 Hz, 2H), 1.67 – 1.53 (m, 4H), 1.49 (m, 2H), 1.28 (m, 5H), 0.94 (t, *J* = 7.1 Hz, 6H).

¹³C NMR (125MHz; DMSO-*d*₆) δ: 171.6, 169.1, 165.5, 141.7, 128.9, 127.8, 118.1, 50.2, 46.3, 38.0, 35.9, 32.2, 28.4, 26.5, 25.0, 24.9, 11.6.

HRMS-ESI(*m/z*) calculated for C₂₂H₃₇N₄O₄ [*M+H*]⁺: 420.2809; Found: 421.2800.

***N*¹-hydroxy-*N*⁸-4-((2-morpholinoethyl)carbamoyl)phenyl)octanediamide (17)** was obtained from 13 (90mg, 0.21mmol) as a white powder (33mg, 0.08mmol, 38%).

¹H NMR (500MHz; DMSO-*d*₆) δ: ¹H NMR (500 MHz, DMSO-*d*₆) δ 10.35 (s, 1H), 10.11 (s, 1H), 8.67 (s, 1H), 8.30 (t, *J* = 5.7 Hz, 1H), 7.77 (d, *J* = 8.4 Hz, 2H), 7.65 (d, *J* = 8.4 Hz, 2H), 3.57 (m, 4H), 3.37 (q, *J* = 6.6 Hz, 2H), 2.50 – 2.40 (m, 6H), 2.31 (t, *J* = 7.4 Hz, 2H), 1.93 (t, *J* = 7.4 Hz, 2H), 1.57 (p, *J* = 7.3 Hz, 2H), 1.48 (p, *J* = 7.3 Hz, 2H), 1.27 (m, 4H).

¹H NMR (500MHz; DMSO-*d*₆) δ: 171.7, 169.2, 165.2, 143.1, 128.7, 128.0, 118.2, 66.0, 56.9, 53.2, 36.4, 36.3, 32.3, 28.4, 25.1, 24.9.

HRMS-ESI(*m/z*) calculated for C₂₁H₃₃N₄O₅ [*M+H*]⁺: 421.1445; Found: 421.2437.

***tert*-Butyl 4-(4-(8-(hydroxyamino)-8-oxooctanamido)benzamido)piperidine-1-carboxylate (18)** was obtained from 14 (100mg, 0.20mmol) as a white powder (69mg, 0.15mmol, 69%).

¹H NMR (600MHz; DMSO-*d*₆) δ: 10.33 (s, 1H), 10.08 (s, 1H), 8.66 (s, 1H), 8.13 (d, *J* = 7.8 Hz, 1H), 7.81 – 7.77 (m, 2H), 7.71 – 7.65 (m, 2H), 4.00 – 3.92 (m, 3H), 2.84 (s, 2H), 2.32 (t, *J* = 7.4 Hz, 2H), 1.94 (t, *J* = 7.3 Hz, 2H), 1.80 – 1.74 (m, 2H), 1.62 – 1.54 (m, 2H), 1.53 – 1.45 (m, 2H), 1.45 – 1.36 (m, 10H), 1.32 – 1.24 (m, 4H).

¹³C (151MHz, DMSO- *d*₆) δ: 172.1, 169.5, 165.4, 154.4, 142.3, 129.2, 128.6, 118.5, 79.1, 46.9, 36.9, 32.7, 31.9, 28.9, 28.9, 28.6, 25.5, 25.4.

HRMS-ESI(*m/z*) calculated for C₂₅H₃₉N₄O₆ [*M+H*]⁺: 491.2864; Found: 491.2856.

Synthesis of *N*¹-hydroxy-*N*⁸-4-(piperidin-4-ylcarbamoyl)phenyl)octanediamide (19)

A solution of 18 (60mg, 0.20mmol) in TFA/DCM 1:2 was stirred at RT overnight. TFA/DCM was evaporated and the residue was purified by reversed phase chromatography using a linear acetonitrile gradient with 0.01% of TEA (0→80% CH₃CN) to afford 19 as a white powder (43mg, 0.11mmol, 31%).

¹H NMR (600MHz; DMSO-*d*₆) δ: 10.07 (s, 1H), 8.09 (d, *J* = 7.8 Hz, 1H), 7.79 (d, *J* = 8.5 Hz, 2H), 7.64 (d, *J* = 8.5 Hz, 2H), 3.84 – 3.76 (m, 1H), 2.98 – 2.91 (m, 2H), 2.49 – 2.46 (m, 2H), 2.32 (t, *J* = 7.4 Hz, 2H), 1.94 (t, *J* = 7.4 Hz, 2H), 1.74 – 1.68 (m, 2H), 1.62 – 1.54 (m, 2H), 1.53 – 1.45 (m, 2H), 1.40 (qd, *J* = 12.0, 4.0 Hz, 2H), 1.33 – 1.23 (m, 4H).

¹³C NMR (151MHz, DMSO- *d*₆) δ: 172.0, 169.5, 165.3, 142.2, 129.4, 128.5, 118.5, 47.8, 45.8, 36.9, 33.4, 32.7, 28.9, 28.9, 25.5, 25.4.

HRMS-ESI(*m/z*) calculated for C₂₀H₃₁N₄O₄ [*M+H*]⁺: 391.2340; Found: 391.2325.

Hydrochloride salt of compounds 4 and 19 were made by precipitation of the title compounds in methanol solution diluted in hydrogen chloride solution (2M). Hydrochloride salt of compound 19 was used for *in vivo* assays.

DMSO solutions of the compounds at 10mM were stocked at -20°C and fresh aliquots were used for the experiments.

Reference drugs SAHA, procainamide, dihydroartemisinin (DHA), chloroquine (CQ), pyrimethamine (PYR), mefloquine (MQ) and monodesethylamodiaquine (desAQ) were purchased from Sigma-Aldrich and diluted in DMSO to 10mM.

Docking studies

AutoDock version 4.2 was used for the docking simulation. The enzyme file was prepared using published coordinates (PDB 5EDU, 4CBT, 2VQV and 5ICN). The Zn metal atom was retained within the protein structures. A charge of +2 and a solvation value of -30 were manually assigned to each Zn atom. The molecule files were built on Biovia Discovery Studio® 4.5 and saved as PDB file. The docking area was assigned visually around the presumed active site. A grid of 36Å × 36Å × 46Å with 0.375Å spacing was calculated around the docking area using AutoGrid.

We selected the Lamarckian genetic algorithm (LGA) for ligand conformational searching, which evaluates a population of possible docking solutions and propagates the most successful individuals from each generation into the subsequent generation of possible solutions.

For each compound, the docking parameters were as follows: trials of 20 dockings, population size of 200, random starting position and conformation, translation step ranges of 1.5Å, rotation step ranges of 35°, elitism of 1, mutation rate of 0.02, crossover rate of 0.8, local search rate of 0.06, and 250000000 energy evaluations.

The docking method was first evaluated by redocking the corresponding ligand of the PDB structure and then docking of the SAHA in the active site. The conformation of the obtained results was inspected and compared to the literature and crystal structures.

The docking results from each of the compounds were clustered on the basis of the root-mean-square deviation (rmsd)

of the Cartesian coordinates of the atoms and were ranked on the basis of free energy of binding. The top-ranked compounds were visually inspected for correct chemical geometry.

Cytotoxicity in the HepG2 and HL60 cell lines

Human HepG2 (hepatocellular carcinoma, DSMZ) and HL60 (acute myeloid leukemia, DSMZ) cells were grown as advised by the provider. Cytotoxicity was evaluated after 72h of drug treatment in 96-well plates by ATPlite (PerkinElmer) according to the manufacturer's protocol. Experiments were run in technical triplicates and at least in two biological replicates. GraphPad Prism 8 was used to interpolate IC₅₀. DMSO was used as control.

P. falciparum Continuous Culture

P. falciparum parasites were cultured using a standard protocol⁵⁵. The laboratory strains used were NF54 and 3D7; *P. falciparum* clinical isolates are described in the relevant section.

Inhibition Activity in the Asexual Stages

IC₅₀ values were obtained as previously described³⁶. Briefly, a range of 7-point and 2-step serial dilutions starting at 500nM were used to assess the activity of the compounds. GraphPad Prism 8 was used to interpolate IC₅₀ from three independent experiments run in triplicate. DHA and DMSO were used as positive and negative controls, respectively.

Stage-Specificity during the Asexual Cell Cycle

Stage-specificity was assessed using previously described methods³⁶. Briefly, asexual NF54 parasites were tightly synchronized (0–3hpi) and incubated for 6h with compound **4** at 3× and 10× IC₅₀ value, at 0, 6, 12, 18, 24, 30, 36, or 42hpi. Following each treatment, cells were pelleted, washed with 10mL of RPMI, and put back into culture in a new plate. Parasitemia was assessed at 72h post-synchronization using Giemsa-stained thin blood smears. The percentage of survival was compared to DMSO-treated parasites. Data were obtained from three independent experiments (one well per condition).

Fixed-Ratio Isobolograms

The effect of the combination of compound **19** with DHA, BIX-01294⁴¹ and compound **70**³⁶ was assessed following the method described by Fivelman *et al*⁴⁰. Briefly, six solutions were prepared containing the following combinations: 5:0, 4:1, 3:2, 2:3, 1:4, and 0:5 (ratios of either DHA, BIX-01294 or **70** mixed with compound **19**). These solutions were 2-step serially diluted, the last row being left for 0.1% DMSO-treated controls. Asynchronous parasite culture containing mostly rings was added at 0.5% parasitemia and 2% final hematocrit. IC₅₀ values were determined after 72h of incubation using the SYBR-green I assay. Fractional IC₅₀ (FIC) values were calculated by dividing the IC₅₀ obtained in the combination by the IC₅₀ obtained with the compound alone. The FIC of each combination was then plotted to obtain the isobologram. The data were obtained in three independent experiments run in triplicate.

In vitro Parasite Reduction Rate (PRR)

The *in vitro* parasite reduction rate was adapted from Sanz *et al*³⁸. 10⁶ infected RBC containing mostly rings were cultivated separately with 10× the IC₅₀ of compounds **4**, **19** or reference drugs (DHA or PYR) for 6h, 24h, 48h, 72h and 96h (0.5% starting parasitemia, 2% hematocrit of *P. falciparum* 3D7). After each incubation time, cells were washed and serially diluted (1/3) with fresh RBC. Growth was assessed after 3 weeks, using the SYBR-green I assay. The number of wells showing parasite growth is correlated to the number of viable parasites at the different time points (as defined by Sanz *et al.*) and allows defining the growth parameters reported in Table 2. The experiment was performed once in duplicate.

Antiplasmodial activity against *P. falciparum* field isolates

P. falciparum isolates used in this study were collected in the framework of the therapeutic efficacy surveillance program in Cambodia between 2017 and 2019. PSA, RSA, AQA and genotyping data have been performed in the Pasteur Institute in Cambodia. Parasites were chosen based on the pattern of multi-drug resistance they carry (10 isolates per type of resistance). IC₅₀ values were obtained as previously described⁴¹ with slight modifications. Ring-synchronized cultures (2% hematocrit, 1% starting parasitemia) were incubated for 96h before growth measurement using the SYBR-green I assay³⁶. A range of 11-point and 2-step serial dilutions, starting at 500nM were used to assess the activity of compounds **4** and **19**. Mefloquine (MQ) and monodesethylamodiaquine (dAQ) were used as positive controls. Experiments were performed in triplicate, with one biological replicate per isolate.

In vivo antimalarial activity

All animal experiments performed in the manuscript were conducted in compliance with French animal welfare laws and Institut Pasteur Animal Care and Use Committee guidelines. *In vivo* activity was determined as previously described³⁹ following the Peters 4-day suppressive test⁵⁶ with slight modifications. 6-weeks old C57BL/6 female mice (Janvier Labs) were infected intraperitoneally (i.p.) with 10⁵ iRBC of *P. berghei* ANKA GFP-expressing parasites⁵⁷. 2h post-infection, mice were treated i.p for 4 days with compound **19** following a regimen of 20mg/kg twice per day, or a daily regimen of 25mg/kg of chloroquine, or the equivalent vehicle control. Parasitemia was quantified from blood samples collected every day by flow cytometry of 200,000 RBCs and confirmed by Giemsa-stained thin blood smears. The experiment was performed once (n=5 mice per group).

Activity against synchronous stage IIb-III and stage IV-V gametocytes

Synchronous gametocytes were induced following previously described methods⁵⁸ with slight modifications. Briefly, trophozoite purification steps were performed using gelatin flotation (Plasmion®). Media containing 0.05% (w/v) Albumax I was used until induction (day 0, corresponding to gametocyte-committed ring stage parasites), followed by a media containing 5% (v/v) human serum and 0.025% (w/v) Albumax I. Asexual parasite populations was removed by *N*-acetyl

Glucosamine treatment for 5 days. Parasites were treated with compounds **4**, **19** and SAHA to evaluate efficacy against early (day 4, stage IIB-III) and late stage gametocytes (day 9, stage IV-V). Parasites, at approximately 1% starting gametocytemia, were seeded in 48-well plates at 2% final hematocrit and treated for 72h with 10, 5, 1, or 0.5 μ M of compounds **4**, **19** or SAHA or with 0.1% DMSO (control). After 72h, gametocytes were washed in prewarmed RPMI and put back into culture in new wells. Afterwards, media was changed daily and the phenotype and parasitemia were examined daily using Giemsa-stained thin blood smears.

Exflagellation assay

Exflagellation of treated stage IV-V gametocytes (as described above) was assessed at day 11 and compared to the DMSO control. Briefly, 5 μ L of the pelleted cells were mixed with 5 μ L of human serum. The mix was mounted on slides and exflagellation centers were counted over at least 10 microscopic fields (objective 40X) in the hour following.

Preparation of HeLa cells nuclear extracts

HeLa cells nuclear extracts were prepared with the NE-PER nuclear and cytoplasmic extraction kit from Thermo Scientific following the manufacturer's protocol.

Preparation of *P. falciparum* extracts

Parasites were tightly synchronized (0-3hpi) and harvested at 12, 24 and 36hpi. Optimal HDAC activity was obtained at trophozoite/schizonts stages, thus asynchronous late stage parasites were collected using gelatin flotation for remaining experiments (HDAC inhibition by the compounds). Cytoplasmic followed by nuclear extraction was carried out by resuspending parasite pellet in cytoplasmic extraction buffer for 5min on ice (20mM HEPES, pH7.9; 10mM KCl; 1mM EDTA, 1mM DTT; 0.65% Igepal; protease inhibitor cocktail, Roche), pelleting the nuclei by centrifugation for 10min at 15000g, 4°C, and resuspending the pellet after washes in the nuclear extraction buffer (20mM HEPES, pH7.9; 100mM NaCl; 0.1mM EDTA, 1.5mM MgCl₂, 1mM DTT; 25% glycerol; protease inhibitor cocktail, Roche). Nuclei were lysed for 20 minutes under vigorous shaking and sonicated for 5 minutes (30sec on/off cycles). Insoluble material was removed by centrifugation at 6000g, 4°C. Protein content was assessed by Bradford quantification. The quality of the nuclear and cytoplasmic extracts was assessed by western blot using Aldolase (Abcam ab38905) and Histone H3 (Abcam ab1791) targeted antibodies.

***In vitro* HDAC enzymatic assay and activity of human and *P. falciparum* protein extracts**

Human HDAC screening was outsourced at Reaction Biology Coop (USA), which uses acetylated substrates for hHDAC1,2,3 and 6 (peptide from p53 residues 379-382 (RHKK(Ac)AMC)), trifluoroacetylated substrate for hHDAC4,5,7, 9 and 11, and double acetylated substrate for HDAC8 (peptide from p53 residues 379-382 (RHK(Ac)K(Ac)AMC)).

IC₅₀ determinations using recombinant hHDACs or HeLa cells and *P. falciparum* protein extracts were performed in house. Test compounds were incubated with 43 μ M of substrate Tosyl-Gly-Pro-Lys(Ac)-AMC in 50 μ L of buffer

(25mM Tris HCl pH 8, 140mM NaCl, 3mM KCl, 1mM MgCl₂) and 3x10⁻³mg of cellular extracts or 130ng/mL of hHDAC1 (Active Motif N°31504) or in 50 μ L of buffer (25mM Tris HCl pH 8, 140mM NaCl, 3mM KCl, 1mM MgCl₂, 1mg/mL BSA, 0.04% Triton X-100, 0.5mM DTT) and 135ng/mL of hHDAC2 (Active Motif N°31909) or 90ng/mL of hHDAC3 (Active Motif N°31609) in Greiner Fluotrac 200 96-well plates. As controls, the substrate alone was incubated in the buffer (background) and DMSO was used to replace the compound for 100% activity. After incubating 45 minutes at 37°C, 20 μ L of trypsin (1mg/mL, SIGMA T1005) was added and incubated 15min at RT. Then 150 μ L of glacial ethanol was added and fluorescence was measured by Perkin Elmer Envision (Peptides AMC excitation at 380nm and emission at 460nm). The specificity of trypsin was measured in the same conditions on substrate Succinyl-Leu-Leu-Arg-AMC. Background was subtracted and data normalized to the DMSO value. Experiments were run in duplicates in at least two independent experiments. GraphPad was used to analyse the data.

***In vitro* hDNMT3a-C and hDNMT1 enzymatic assay and activity of *P. falciparum* protein extracts**

Activity against human DNMTs was performed as previously described⁵⁹ and developed by Ceccaldi *et al*⁶⁰. Assay was performed on *P. falciparum* extracts following methods described in Nardella *et al*³⁶ at a concentration of 32 μ M of compound **4**, DHA, or the equivalent amount of DMSO. Data were run in triplicate in 2 independent experiments and are normalized to the DMSO sample.

Western blotting of treated parasites

Parasites were incubated for 4h with 10X the IC₅₀ of either SAHA, compound **4**, compound **19**, CQ or 0.1% DMSO, and harvested using 0.15% saponin lysis followed by multiple washes with cold PBS. Parasite pellets were then extracted using lysis buffer (10 μ L per 10⁷ parasites: 1mM DTT, 2X Laemmli buffer, and protease inhibitors dissolved in PBS). 5.10⁶ parasites were loaded per lane in a 4-15% TGX Stain-Free gel (Biorad) and proteins were transferred onto a nitrocellulose membrane. Subsequent steps were performed in PBS containing 0.01% Tween-20 and 5% skim milk. Anti-H3 was diluted 1/1000 (Abcam ab1791) and anti-H4K16Ac was diluted 1/500 (Abcam ab1762); secondary anti-rabbit HRP antibody was used at 1/2000. The blot was revealed using Super Signal West-Pico (H3) or Femto (H4K16Ac) chemiluminescent substrate (Thermo Fisher Scientific). Band intensity of H4K16Ac was normalized to H3 (loading control) using ImageLab (Biorad). Data were obtained from three independent experiments. Figure 1c shows the membrane of one representative experiment.

Samples preparation for Transmission Electron Microscopy

Ring-stage parasite (0-12h window) were treated for 24h at a concentration corresponding to 10x the IC₅₀ of compound **4** or 0.1% DMSO. After 24h, parasites were harvested using Plasmagel and fixed in 4% PFA containing 0.1% Glutaraldehyde. Samples were then embedded in gelatin and treated following published methods^{61,62}. Ultrathin sections of 60nm were obtained (Leica FC-6) and deposited onto grids. For Histone 3 staining, sections were

blocked 30 min in PBS containing 5% skim milk and 0.01% Tween-20. The grids were incubated for 1h in rabbit anti-Histone 3 diluted 1/100 (abcam, ab1791) in PBS containing 1% BSA (fraction V) and 0.01% Tween-20. The grids were washed 5 times in PBS containing 0.1% BSA (fraction V). Antibodies were labelled with 10nm protein A-colloidal gold (Cell Microscopy Center, University Medical Center Utrecht, The Netherlands) for 25 minutes. Washed sections were stained 5 minutes with methylcellulose containing 0.4% uranyl acetate. Sections were analysed by electron microscopy at 120 kV (Tecnai biotwin 120 FEI).

Microsomal and plasma stability

Rat and human microsomal stability and plasma stability were outsourced at Fidelta Ltd., Zagreb, Croatia.

ANCILLARY INFORMATION

ASSOCIATED CONTENT

Supporting Information.

Docking studies of lead compound **19** compared to SAHA in the catalytic pocket of hHDAC1, hHDAC4 and hHDAC6 are shown in 3D and 2D representation in the Supplementary data, as well as HPLC traces for lead compounds.

Molecular formula strings

Molecular formula strings and SAR data are available as additional CSV file.

AUTHOR INFORMATION

Corresponding Author

* authors to whom correspondence should be addressed: Artur Scherf (artur.scherf@pasteur.fr) and Paola B. Arimondo (paola.arimondo@cnrs.fr).

Author Contributions

The manuscript was written through contributions of all authors. All authors have given approval to the final version of the manuscript. ‡These authors contributed equally.

Funding Sources

This work was supported by Innovation program by Institut Pasteur-Institut Carnot (S-CR18089-02B15 DARRI CONSO INNOV 46-19; S-PI15006-10A INNOV 05-2019 ARIMONDO IARP 2019-PC), Pasteur Transversal Research Program (PTR 233-2019 HALBY), and Pasteur Swiss Foundation grant.

ACKNOWLEDGMENT

We thank Bruno Vitorge from the Institut Pasteur Biological NMR Technological Platform for help with NMR experiments, Frédéric Bonhomme of the CNRS-Institut Pasteur UMR3523 Organic Chemistry Unit for assisting with HRMS analysis and Sophie Vichier-Guerre of the Chemistry and Biocatalysis Unit (Institut Pasteur-CNRS) for HPLC analysis. We thank Patty Chen proof reading.

ABBREVIATIONS

ACT, artemisinin-based combination therapies; PTM, post-translational modifications; HAT, histone-acetyl-transferase; HDAC, histone deacetylase; DNMT, DNA methyltransferase; SAR: structure-activity relationship study; SAHA: SuberoylAnilide Hydroxamic Acid; IDC, intra-erythrocytic developmental cycle; DHA, dihydroartemisinin; CQ, chloroquine; PYR, pyrimethamine; MQ, mefloquine; PPQ,

piperaquine; AQ/desAQ, (monodesethyl)amodiaquine; RBC, red blood cell; Kn, knob; Mc, Maurer clefts; Pv, parasitophorous vacuole; Hz, hemozoin crystals; N, nucleus; Rh, rhoptry .

REFERENCES

- (1) World Health Organisation. *World Malaria Report 2020*; Global Malaria Programme, WHO Global, 2020; p 19.
- (2) Vandoolaeghe, P.; Schuerman, L. The RTS,S/AS01 Malaria Vaccine in Children 5 to 17 Months of Age at First Vaccination. *Expert Rev. Vaccines* **2016**, *15* (12), 1481–1493. <https://doi.org/10.1080/14760584.2016.1236689>.
- (3) Churcher, T. S.; Lissenden, N.; Griffin, J. T.; Worrall, E.; Ranson, H. The Impact of Pyrethroid Resistance on the Efficacy and Effectiveness of Bednets for Malaria Control in Africa. *eLife* **2016**, *5*. <https://doi.org/10.7554/eLife.16090>.
- (4) Leang, R.; Taylor, W. R. J.; Bouth, D. M.; Song, L.; Tarning, J.; Char, M. C.; Kim, S.; Witkowski, B.; Duru, V.; Domergue, A.; Khim, N.; Ringwald, P.; Menard, D. Evidence of Falciparum Malaria Multidrug Resistance to Artemisinin and Piperaquine in Western Cambodia: Dihydroartemisinin-Piperaquine Open-Label Multi-center Clinical Assessment. *Antimicrob. Agents Chemother.* **2015**. <https://doi.org/10.1128/AAC.00835-15>.
- (5) Duru, V.; Khim, N.; Leang, R.; Kim, S.; Domergue, A.; Kloeung, N.; Ke, S.; Chy, S.; Eam, R.; Khean, C.; Loch, K.; Ken, M.; Lek, D.; Beghain, J.; Arie, F.; Guerin, P. J.; Huy, R.; Mercereau-Puijalon, O.; Witkowski, B.; Menard, D. Plasmodium Falciparum Dihydroartemisinin-Piperaquine Failures in Cambodia Are Associated with Mutant K13 Parasites Presenting High Survival Rates in Novel Piperaquine in Vitro Assays: Retrospective and Prospective Investigations. *BMC Med.* **2015**, *13* (1). <https://doi.org/10.1186/s12916-015-0539-5>.
- (6) Menard, D.; Dondorp, A. Antimalarial Drug Resistance: A Threat to Malaria Elimination. *Cold Spring Harb. Perspect. Med.* **2017**, *7* (7). <https://doi.org/10.1101/cshperspect.a025619>.
- (7) Mairet-Khedim, M.; Leang, R.; Marmai, C.; Khim, N.; Kim, S.; Ke, S.; Kaoy, C.; Kloeung, N.; Eam, R.; Chy, S.; Izac, B.; Bouth, D. M.; Bustos, M. D.; Ringwald, P.; Arie, F.; Witkowski, B. Clinical and in Vitro Resistance of Plasmodium Falciparum to Artesunate-Amodiaquine in Cambodia. *Clin. Infect. Dis.* <https://doi.org/10.1093/cid/ciaa628>.
- (8) Doerig, C.; Rayner, J. C.; Scherf, A.; Tobin, A. B. Post-Translational Protein Modifications in Malaria Parasites. *Nat. Rev. Microbiol.* **2015**, *13* (3), 160–172. <https://doi.org/10.1038/nrmicro3402>.
- (9) Castillo-Aguilera, O.; Depreux, P.; Halby, L.; Arimondo, P. B.; Goossens, L. DNA Methylation Targeting: The DNMT/HMT Crosstalk Challenge. *Biomolecules* **2017**, *7* (1). <https://doi.org/10.3390/biom7010003>.
- (10) Lopez, M.; Halby, L.; Arimondo, P. B. DNA Methyltransferase Inhibitors: Development and Applications. *Adv. Exp. Med. Biol.* **2016**, *945*, 431–473. https://doi.org/10.1007/978-3-319-43624-1_16.
- (11) Fioravanti, R.; Mautone, N.; Rovere, A.; Rotili, D.; Mai, A. Targeting Histone Acetylation/Deacetylation in Parasites: An Update (2017-2020). *Curr. Opin. Chem.*

- Biol.* **2020**, *57*, 65–74. <https://doi.org/10.1016/j.cbpa.2020.05.008>.
- (12) Kanyal, A.; Rawat, M.; Gurung, P.; Choubey, D.; Anamika, K.; Karmodiya, K. Genome-Wide Survey and Phylogenetic Analysis of Histone Acetyltransferases and Histone Deacetylases of *Plasmodium Falciparum*. *FEBS J.* **2018**, *285* (10), 1767–1782. <https://doi.org/10.1111/febs.14376>.
- (13) Joshi, M. B.; Lin, D. T.; Chiang, P. H.; Goldman, N. D.; Fujioka, H.; Aikawa, M.; Syin, C. Molecular Cloning and Nuclear Localization of a Histone Deacetylase Homologue in *Plasmodium Falciparum*. *Mol. Biochem. Parasitol.* **1999**, *99* (1), 11–19. [https://doi.org/10.1016/S0166-6851\(98\)00177-7](https://doi.org/10.1016/S0166-6851(98)00177-7).
- (14) Chaal, B. K.; Gupta, A. P.; Wastuwidyaningtyas, B. D.; Luah, Y.-H.; Bozdech, Z. Histone Deacetylases Play a Major Role in the Transcriptional Regulation of the *Plasmodium Falciparum* Life Cycle. *PLoS Pathog.* **2010**, *6* (1), e1000737. <https://doi.org/10.1371/journal.ppat.1000737>.
- (15) Engel, J. A.; Norris, E. L.; Gilson, P.; Przyborski, J.; Shonhai, A.; Blatch, G. L.; Skinner-Adams, T. S.; Gorman, J.; Headlam, M.; Andrews, K. T. Proteomic Analysis of *Plasmodium Falciparum* Histone Deacetylase 1 Complex Proteins. *Exp. Parasitol.* **2019**, *198*, 7–16. <https://doi.org/10.1016/j.exppara.2019.01.008>.
- (16) Coleman, B. I.; Skillman, K. M.; Jiang, R. H. Y.; Childs, L. M.; Altenhofen, L. M.; Ganter, M.; Leung, Y.; Goldowitz, I.; Kafsack, B. F. C.; Marti, M.; Llinás, M.; Buckee, C. O.; Duraisingh, M. T. A *Plasmodium Falciparum* Histone Deacetylase Regulates Antigenic Variation and Gametocyte Conversion. *Cell Host Microbe* **2014**, *16* (2), 177–186. <https://doi.org/10.1016/j.chom.2014.06.014>.
- (17) Freitas-Junior, L. H.; Hernandez-Rivas, R.; Ralph, S. A.; Montiel-Condado, D.; Ruvalcaba-Salazar, O. K.; Rojas-Meza, A. P.; Mâncio-Silva, L.; Leal-Silvestre, R. J.; Gontijo, A. M.; Shorte, S.; Scherf, A. Telomeric Heterochromatin Propagation and Histone Acetylation Control Mutually Exclusive Expression of Antigenic Variation Genes in Malaria Parasites. *Cell* **2005**, *121* (1), 25–36. <https://doi.org/10.1016/j.cell.2005.01.037>.
- (18) Duraisingh, M. T.; Voss, T. S.; Marty, A. J.; Duffy, M. F.; Good, R. T.; Thompson, J. K.; Freitas-Junior, L. H.; Scherf, A.; Crabb, B. S.; Cowman, A. F. Heterochromatin Silencing and Locus Repositioning Linked to Regulation of Virulence Genes in *Plasmodium Falciparum*. *Cell* **2005**, *121* (1), 13–24. <https://doi.org/10.1016/j.cell.2005.01.036>.
- (19) Tonkin, C. J.; Carret, C. K.; Duraisingh, M. T.; Voss, T. S.; Ralph, S. A.; Hommel, M.; Duffy, M. F.; Silva, L. M. da; Scherf, A.; Ivens, A.; Speed, T. P.; Beeson, J. G.; Cowman, A. F. Sir2 Paralogues Cooperate to Regulate Virulence Genes and Antigenic Variation in *Plasmodium Falciparum*. *PLoS Biol.* **2009**, *7* (4), e84. <https://doi.org/10.1371/journal.pbio.1000084>.
- (20) Wang, Q.; Rosa, B. A.; Nare, B.; Powell, K.; Valente, S.; Rotili, D.; Mai, A.; Marshall, G. R.; Mitreva, M. Targeting Lysine Deacetylases (KDACs) in Parasites. *PLoS Negl. Trop. Dis.* **2015**, *9* (9), e0004026. <https://doi.org/10.1371/journal.pntd.0004026>.
- (21) Hailu, G. S.; Robaa, D.; Forgione, M.; Sippl, W.; Rotili, D.; Mai, A. Lysine Deacetylase Inhibitors in Parasites: Past, Present, and Future Perspectives. *J. Med. Chem.* **2017**, *60* (12), 4780–4804. <https://doi.org/10.1021/acs.jmedchem.6b01595>.
- (22) Andrews, K. T.; Walduck, A.; Kelso, M. J.; Fairlie, D. P.; Saul, A.; Parsons, P. G. Anti-Malarial Effect of Histone Deacetylation Inhibitors and Mammalian Tumour Cytodifferentiating Agents. *Int. J. Parasitol.* **2000**, *8*.
- (23) Dow, G. S.; Chen, Y.; Andrews, K. T.; Caridha, D.; Gerena, L.; Gettayacamin, M.; Johnson, J.; Li, Q.; Melendez, V.; Obaldia, N.; Tran, T. N.; Kozikowski, A. P. Antimalarial Activity of Phenylthiazolyl-Bearing Hydroxamate-Based Histone Deacetylase Inhibitors. *Antimicrob. Agents Chemother.* **2008**, *52* (10), 3467–3477. <https://doi.org/10.1128/AAC.00439-08>.
- (24) Sumanadasa, S. D. M.; Goodman, C. D.; Lucke, A. J.; Skinner-Adams, T.; Sahama, I.; Haque, A.; Do, T. A.; McFadden, G. I.; Fairlie, D. P.; Andrews, K. T. Antimalarial Activity of the Anticancer Histone Deacetylase Inhibitor SB939. *Antimicrob. Agents Chemother.* **2012**, *56* (7), 3849–3856. <https://doi.org/10.1128/AAC.00030-12>.
- (25) Hansen, F. K.; Sumanadasa, S. D. M.; Stenzel, K.; Duffy, S.; Meister, S.; Marek, L.; Schmetter, R.; Kuna, K.; Hamacher, A.; Mordmüller, B.; Kassack, M. U.; Winzeler, E. A.; Avery, V. M.; Andrews, K. T.; Kurz, T. Discovery of HDAC Inhibitors with Potent Activity against Multiple Malaria Parasite Life Cycle Stages. *Eur. J. Med. Chem.* **2014**, *82*, 204–213. <https://doi.org/10.1016/j.ejmech.2014.05.050>.
- (26) Hansen, F. K.; Skinner-Adams, T. S.; Duffy, S.; Marek, L.; Sumanadasa, S. D. M.; Kuna, K.; Held, J.; Avery, V. M.; Andrews, K. T.; Kurz, T. Synthesis, Antimalarial Properties, and SAR Studies of Alkoxyurea-Based HDAC Inhibitors. *ChemMedChem* **2014**, *9* (3), 665–670. <https://doi.org/10.1002/cmdc.201300469>.
- (27) Giannini, G.; Battistuzzi, G.; Vignola, D. Hydroxamic Acid Based Histone Deacetylase Inhibitors with Confirmed Activity against the Malaria Parasite. *Bioorg. Med. Chem. Lett.* **2015**, *25* (3), 459–461. <https://doi.org/10.1016/j.bmcl.2014.12.051>.
- (28) Stenzel, K.; Chua, M. J.; Duffy, S.; Antonova-Koch, Y.; Meister, S.; Hamacher, A.; Kassack, M. U.; Winzeler, E.; Avery, V. M.; Kurz, T.; Andrews, K. T.; Hansen, F. K. Design and Synthesis of Terephthalic Acid-Based Histone Deacetylase Inhibitors with Dual-Stage Anti-*Plasmodium* Activity. *ChemMedChem* **2017**, *12* (19), 1627–1636. <https://doi.org/10.1002/cmdc.201700360>.
- (29) Diedrich, D.; Stenzel, K.; Hespings, E.; Antonova-Koch, Y.; Gebru, T.; Duffy, S.; Fisher, G.; Schöler, A.; Meister, S.; Kurz, T.; Avery, V. M.; Winzeler, E. A.; Held, J.; Andrews, K. T.; Hansen, F. K. One-Pot, Multi-Component Synthesis and Structure-Activity Relationships of Peptoid-Based Histone Deacetylase (HDAC) Inhibitors Targeting Malaria Parasites. *Eur. J. Med. Chem.* **2018**, *158*, 801–813. <https://doi.org/10.1016/j.ejmech.2018.09.018>.
- (30) Mackwitz, M. K. W.; Hespings, E.; Antonova-Koch, Y.; Diedrich, D.; Woldearegai, T. G.; Skinner-Adams, T.; Clarke, M.; Schöler, A.; Limbach, L.; Kurz, T.; Winzeler, E. A.; Held, J.; Andrews, K. T.; Hansen, F. K. Structure-Activity and Structure-Toxicity Relationships of Peptoid-Based Histone Deacetylase Inhibitors with Dual-Stage Antiplasmodial Activity. *ChemMedChem* **2019**, *14* (9), 912–926. <https://doi.org/10.1002/cmdc.201800808>.

- (31) de Lera, A. R.; Ganesan, A. Epigenetic Polypharmacology: From Combination Therapy to Multitargeted Drugs. *Clin. Epigenetics* **2016**, *8*, 105. <https://doi.org/10.1186/s13148-016-0271-9>.
- (32) Ganesan, A. Multitarget Drugs: An Epigenetic Epiphany. *ChemMedChem* **2016**, *11* (12), 1227–1241. <https://doi.org/10.1002/cmdc.201500394>.
- (33) Marchi, E.; Zullo, K. M.; Amengual, J. E.; Kalac, M.; Bongero, D.; McIntosh, C. M.; Fogli, L. K.; Rossi, M.; Zinzani, P. L.; Pileri, S. A.; Piccaluga, P. P.; Fuligni, F.; Scotto, L.; O'Connor, O. A. The Combination of Hypomethylating Agents and Histone Deacetylase Inhibitors Produce Marked Synergy in Preclinical Models of T-Cell Lymphoma. *Br. J. Haematol.* **2015**, *171* (2), 215–226. <https://doi.org/10.1111/bjh.13566>.
- (34) Juergens, R. A.; Wrangle, J.; Vendetti, F. P.; Murphy, S. C.; Zhao, M.; Coleman, B.; Sebre, R.; Rodgers, K.; Hooker, C. M.; Franco, N.; Lee, B.; Tsai, S.; Delgado, I. E.; Rudek, M. A.; Belinsky, S. A.; Herman, J. G.; Baylin, S. B.; Brock, M. V.; Rudin, C. M. Combination Epigenetic Therapy Has Efficacy in Patients with Refractory Advanced Non-Small Cell Lung Cancer. *Cancer Discov.* **2011**. <https://doi.org/10.1158/2159-8290.CD-11-0214>.
- (35) Bouchut, A.; Rotili, D.; Pierrot, C.; Valente, S.; Lafitte, S.; Schultz, J.; Hoglund, U.; Mazzone, R.; Lucidi, A.; Fabrizi, G.; Pechalrieu, D.; Arimondo, P. B.; Skinner-Adams, T. S.; Chua, M. J.; Andrews, K. T.; Mai, A.; Khalife, J. Identification of Novel Quinazoline Derivatives as Potent Antiplasmodial Agents. *Eur. J. Med. Chem.* **2019**, *161*, 277–291. <https://doi.org/10.1016/j.ejmech.2018.10.041>.
- (36) Nardella, F.; Halby, L.; Hammam, E.; Erdmann, D.; Cadet-Daniel, V.; Peronet, R.; Ménard, D.; Witkowski, B.; Mecheri, S.; Scherf, A.; Arimondo, P. B. DNA Methylation Bisubstrate Inhibitors Are Fast-Acting Drugs Active against Artemisinin-Resistant Plasmodium Falciparum Parasites. *ACS Cent. Sci.* **2020**, *6* (1), 16–21. <https://doi.org/10.1021/acscentsci.9b00874>.
- (37) Lee, B. H.; Yegnasubramanian, S.; Lin, X.; Nelson, W. G. Procainamide Is a Specific Inhibitor of DNA Methyltransferase 1. *J. Biol. Chem.* **2005**, *280* (49), 40749–40756. <https://doi.org/10.1074/jbc.M505593200>.
- (38) Sanz, L. M.; Crespo, B.; De-Cózar, C.; Ding, X. C.; Llergo, J. L.; Burrows, J. N.; García-Bustos, J. F.; Gamo, F.-J. P. Falciparum In Vitro Killing Rates Allow to Discriminate between Different Antimalarial Mode-of-Action. *PLoS ONE* **2012**, *7* (2), e30949. <https://doi.org/10.1371/journal.pone.0030949>.
- (39) Malmquist, N. A.; Sundriyal, S.; Caron, J.; Chen, P.; Witkowski, B.; Menard, D.; Suwanarusk, R.; Renia, L.; Nosten, F.; Jiménez-Díaz, M. B.; Angulo-Barturen, I.; Santos Martínez, M.; Ferrer, S.; Sanz, L. M.; Gamo, F.-J.; Wittlin, S.; Duffy, S.; Avery, V. M.; Ruecker, A.; Delves, M. J.; Sinden, R. E.; Fuchter, M. J.; Scherf, A. Histone Methyltransferase Inhibitors Are Orally Bioavailable, Fast-Acting Molecules with Activity against Different Species Causing Malaria in Humans. *Antimicrob. Agents Chemother.* **2015**, *59* (2), 950–959. <https://doi.org/10.1128/AAC.04419-14>.
- (40) Fivelman, Q. L.; Adagu, I. S.; Warhurst, D. C. Modified Fixed-Ratio Isobologram Method for Studying In Vitro Interactions between Atovaquone and Proguanil or Dihydroartemisinin against Drug-Resistant Strains of Plasmodium Falciparum. *Antimicrob. Agents Chemother.* **2004**, *48* (11), 4097–4102. <https://doi.org/10.1128/AAC.48.11.4097-4102.2004>.
- (41) Malmquist, N. A.; Moss, T. A.; Mecheri, S.; Scherf, A.; Fuchter, M. J. Small-Molecule Histone Methyltransferase Inhibitors Display Rapid Antimalarial Activity against All Blood Stage Forms in Plasmodium Falciparum. *Proc. Natl. Acad. Sci.* **2012**, *109* (41), 16708–16713. <https://doi.org/10.1073/pnas.1205414109>.
- (42) Vanheer, L. N.; Zhang, H.; Lin, G.; Kafsack, B. F. C. Activity of Epigenetic Inhibitors against Plasmodium Falciparum Asexual and Sexual Blood Stages. *Antimicrob. Agents Chemother.* **2020**, *64* (7), 6.
- (43) Coetzee, N.; von Grüning, H.; Opperman, D.; van der Watt, M.; Reader, J.; Birkholtz, L.-M. Epigenetic Inhibitors Target Multiple Stages of Plasmodium Falciparum Parasites. *Sci. Rep.* **2020**, *10* (1), 2355. <https://doi.org/10.1038/s41598-020-59298-4>.
- (44) Soumyanarayanan, U.; Ramanujulu, P. M.; Mustafa, N.; Haider, S.; Fang Nee, A. H.; Tong, J. X.; Tan, K. S. W.; Chng, W. J.; Dymock, B. W. Discovery of a Potent Histone Deacetylase (HDAC) 3/6 Selective Dual Inhibitor. *Eur. J. Med. Chem.* **2019**, *184*, 111755. <https://doi.org/10.1016/j.ejmech.2019.111755>.
- (45) Chua, M. J.; Arnold, M. S. J.; Xu, W.; Lancelot, J.; Lamotte, S.; Späth, G. F.; Prina, E.; Pierce, R. J.; Fairlie, D. P.; Skinner-Adams, T. S.; Andrews, K. T. Effect of Clinically Approved HDAC Inhibitors on Plasmodium, Leishmania and Schistosoma Parasite Growth. *Int. J. Parasitol. Drugs Drug Resist.* **2017**, *7* (1), 42–50. <https://doi.org/10.1016/j.ijpddr.2016.12.005>.
- (46) Koehne, E.; Kreidenweiss, A.; Zoleko Manego, R.; McCall, M.; Mombo-Ngoma, G.; Mackwitz, M. K. W.; Hansen, F. K.; Held, J. Histone Deacetylase Inhibitors with High in Vitro Activities against Plasmodium Falciparum Isolates Collected from Gabonese Children and Adults. *Sci. Rep.* **2019**, *9*. <https://doi.org/10.1038/s41598-019-53912-w>.
- (47) Vreese, R. D.; Kock, C. de; Smith, P. J.; Chibale, K.; D'hooghe, M. Exploration of Thiaheterocyclic HHDAC6 Inhibitors as Potential Antiplasmodial Agents. *Future Med. Chem.* **2017**, *9* (4), 357–364. <https://doi.org/10.4155/fmc-2016-0215>.
- (48) Melesina, J.; Robaa, D.; Pierce, R. J.; Romier, C.; Sippl, W. Homology Modeling of Parasite Histone Deacetylases to Guide the Structure-Based Design of Selective Inhibitors. *J. Mol. Graph. Model.* **2015**, *62*, 342–361. <https://doi.org/10.1016/j.jmgm.2015.10.006>.
- (49) Hubbert, C.; Guardiola, A.; Shao, R.; Kawaguchi, Y.; Ito, A.; Nixon, A.; Yoshida, M.; Wang, X.-F.; Yao, T.-P. HDAC6 Is a Microtubule-Associated Deacetylase. *Nature* **2002**, *417* (6887), 455–458. <https://doi.org/10.1038/417455a>.
- (50) Skultetyova, L.; Ustinova, K.; Kutil, Z.; Novakova, Z.; Pavlicek, J.; Mikesova, J.; Trapl, D.; Baranova, P.; Havlinova, B.; Hubalek, M.; Lansky, Z.; Barinka, C. Human Histone Deacetylase 6 Shows Strong Preference for Tubulin Dimers over Assembled Microtubules. *Sci. Rep.* **2017**, *7* (1), 11547. <https://doi.org/10.1038/s41598-017-11739-3>.
- (51) Dixon, M. W. A.; Dearnley, M. K.; Hanssen, E.; Gilberger, T.; Tilley, L. Shape-Shifting Gametocytes: How and Why Does P. Falciparum Go Banana-Shaped?

- Trends Parasitol.* **2012**, *28* (11), 471–478. <https://doi.org/10.1016/j.pt.2012.07.007>.
- (52) Marfurt, J.; Chalfein, F.; Prayoga, P.; Wabiser, F.; Kenangalem, E.; Piera, K. A.; Fairlie, D. P.; Tjitra, E.; Anstey, N. M.; Andrews, K. T.; Price, R. N. Ex Vivo Activity of Histone Deacetylase Inhibitors against Multi-drug-Resistant Clinical Isolates of Plasmodium Falciparum and P. Vivax. *Antimicrob. Agents Chemother.* **2011**, *55* (3), 961–966. <https://doi.org/10.1128/AAC.01220-10>.
- (53) Mok, S.; Imwong, M.; Mackinnon, M. J.; Sim, J.; Ramadoss, R.; Yi, P.; Mayxay, M.; Chotivanich, K.; Liong, K.-Y.; Russell, B.; Socheat, D.; Newton, P. N.; Day, N. P. J.; White, N. J.; Preiser, P. R.; Nosten, F.; Dondorp, A. M.; Bozdech, Z. Artemisinin Resistance in Plasmodium Falciparum Is Associated with an Altered Temporal Pattern of Transcription. *BMC Genomics* **2011**, *12*, 391. <https://doi.org/10.1186/1471-2164-12-391>.
- (54) Trenholme, K.; Marek, L.; Duffy, S.; Pradel, G.; Fisher, G.; Hansen, F. K.; Skinner-Adams, T. S.; Butterworth, A.; Ngwa, C. J.; Moecking, J.; Goodman, C. D.; McFadden, G. I.; Sumanadasa, S. D. M.; Fairlie, D. P.; Avery, V. M.; Kurz, T.; Andrews, K. T. Lysine Acetylation in Sexual Stage Malaria Parasites Is a Target for Antimalarial Small Molecules. *Antimicrob. Agents Chemother.* **2014**, *58* (7), 3666–3678. <https://doi.org/10.1128/AAC.02721-13>.
- (55) Trager, W.; Jensen, J. B. Human Malaria Parasites in Continuous Culture. *Science* **1976**, *193* (4254), 673–675.
- (56) Peters, W. The Chemotherapy of Rodent Malaria, XXII. The Value of Drug-Resistant Strains of P. Berghei in Screening for Blood Schizontocidal Activity. *Ann. Trop. Med. Parasitol.* **1975**, *69* (2), 155–171.
- (57) Ishino, T.; Orito, Y.; Chinzei, Y.; Yuda, M. A Calcium-Dependent Protein Kinase Regulates Plasmodium Ookinete Access to the Midgut Epithelial Cell. *Mol. Microbiol.* **2006**, *59* (4), 1175–1184. <https://doi.org/10.1111/j.1365-2958.2005.05014.x>.
- (58) Duffy, S.; Loganathan, S.; Holleran, J. P.; Avery, V. M. Large-Scale Production of Plasmodium Falciparum Gametocytes for Malaria Drug Discovery. *Nat. Protoc.* **2016**, *11* (5), 976–992. <https://doi.org/10.1038/nprot.2016.056>.
- (59) Gros, C.; Chauvigné, L.; Poulet, A.; Menon, Y.; Ausseil, F.; Dufau, I.; Arimondo, P. B. Development of a Universal Radioactive DNA Methyltransferase Inhibition Test for High-Throughput Screening and Mechanistic Studies. *Nucleic Acids Res.* **2013**, *41* (19), e185. <https://doi.org/10.1093/nar/gkt753>.
- (60) Ceccaldi, A.; Rajavelu, A.; Champion, C.; Rampon, C.; Jurkowska, R.; Jankevicius, G.; Sénamaud-Beaufort, C.; Ponger, L.; Gagey, N.; Ali, H. D.; Tost, J.; Vríz, S.; Ros, S.; Dauzonne, D.; Jeltsch, A.; Guianvarc’h, D.; Arimondo, P. B. C5-DNA Methyltransferase Inhibitors: From Screening to Effects on Zebrafish Embryo Development. *Chembiochem Eur. J. Chem. Biol.* **2011**, *12* (9), 1337–1345. <https://doi.org/10.1002/cbic.201100130>.
- (61) Tokuyasu, K. T. A Technique for Ultracryotomy of Cell Suspensions and Tissues. *J. Cell Biol.* **1973**, *57* (2), 551–565. <https://doi.org/10.1083/jcb.57.2.551>.
- (62) Slot, J. W.; Geuze, H. J. Cryosectioning and Immunolabeling. *Nat. Protoc.* **2007**, *2* (10), 2480–2491. <https://doi.org/10.1038/nprot.2007.365>.

Table of Contents Graphic

